Does a bottom-up mechanism promote hypoxia in the Mississippi Bight?

Virginie Sanial, Willard S Moore, Alan M Shiller

Marine Chemistry 235 (2021) 104007

Contents lists available at ScienceDirect

Marine Chemistry

journal homepage: www.elsevier.com/locate/marchem

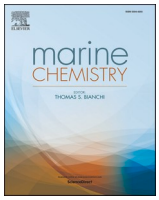

Does a bottom-up mechanism promote hypoxia in the Mississippi Bight?

Virginie Sanial [a,1], Willard S. Moore [b], Alan M. Shiller [a,*]

[a] School of Ocean Science and Engineering, University of Southern Mississippi, 1020 Balch Blvd., Stennis Space Center, MS 39529, USA
[b] School of Earth, Ocean and Environmental Science, University of South Carolina, Columbia, SC, USA

ARTICLE INFO

Keywords:
Hypoxia
Mississippi Bight
Submarine groundwater discharge
Ra isotopes
Nutrients

ABSTRACT

The Mississippi Bight, east of the Mississippi River, is a complex coastal ecosystem that, like the better-known Louisiana Shelf to the west, experiences seasonal bottom water hypoxia. However, input of allochthonous nutrients from the Mississippi River to the Mississippi Bight appears to be limited, begging the question of what drives seasonal hypoxia in this system. Prior research has suggested submarine groundwater discharge (SGD) could be an overlooked component of the Mississippi Bight biogeochemical system. We thus examined the hypothesis that SGD provides a "bottom up" driver for seasonal hypoxia in this area. We used a multi-tracer approach based on known SGD indicators (dissolved Ra, Ba, Si, methane) to: i) demonstrate the presence of SGD as a constituent contributor to Bight bottom waters, ii) constrain the SGD flux of macronutrients, and, iii) investigate the hypoxia-SGD linkage. We found excess SGD tracers in saline bottom waters relative to surface waters, suggesting a bottom source. Examination of other sources for the constituent enrichments besides SGD (e.g., rivers, produced waters from oil wells) appear inadequate to close the bottom water chemical mass balances. Additionally, inverse correlations between DO and SGD indicators in bottom waters support a common mechanism supplying dissolved Ra, Ba, and Si, and decreasing DO concentrations in these waters. Two different approaches to modeling the bottom water Ra distribution both suggest a seepage rate of ~0.055 $m^3\ m^{-2}\ d^{-1}$, in line with previous estimates in similar systems. Our more complex model, involving four mass balances, suggests that as much as 10–20% of the bottom water in the Bight circulates through the underlying permeable sediments on a time scale of ~10 days. This circulated water emerges as SGD with completely altered chemistry. More specifically, SGD appears in some cases to be the dominant contributor of nutrients to Bight bottom waters. Additionally, the potential oxygen demand of reduced species within SGD likely contributes significantly to the development of seasonal hypoxia in Bight bottom waters. Further work is needed to better resolve sources of nutrients and additional reduced species within the Mississippi Bight SGD as well as the variability and pathways of this supply. Nonetheless, the bottom-up influence of SGD on the Mississippi Bight appears to be a significant and overlooked aspect of this system. We suggest that such a bottom-up influence may be a generally important feature of coastal ecosystems.

1. Introduction

Coastal hypoxia is usually defined by dissolved oxygen (DO) concentrations low enough to be deleterious to fish and invertebrates, and is often operationally identified by DO <2 mg L^{-1} or 63 μM (Vaquer-Sunyer and Duarte, 2008). Coastal hypoxia is of global concern and appears to be expanding: over 500 coastal areas have reported low DO, yet this phenomenon was reported in less than 10% of these regions before 1950 (Breitburg et al., 2018; Diaz and Rosenberg, 1995; Selman et al., 2008). Two recognized factors lead to coastal hypoxia: a) a limited rate of DO supply, usually caused by stratification, and b) enhanced DO consumption, often attributed to respiration of organic matter created by the supply of allochthonous nutrients (e.g., Diaz, 2001). This input of allochthonous nutrients to coastal/estuarine surface waters stimulates the biological production of organic matter, which is then exported to semi-isolated bottom waters to fuel respiration; this might be termed a "top-down" delivery of oxygen-depleting species. However, recent work suggests an additional "bottom-up" delivery of anoxic water by saline submarine groundwater discharge (SGD) directly into bottom waters that can also trigger coastal hypoxia (Peterson et al., 2016). The

* Corresponding author.
E-mail address: alan.shiller@usm.edu (A.M. Shiller).
[1] Now at: Univ. Toulon, Aix Marseille Univ., CNRS/INSU, IRD, Mediterranean Institute of Oceanography UM 110, CS 60584 Toulon 83041

https://doi.org/10.1016/j.marchem.2021.104007
Received 7 January 2021; Received in revised form 9 June 2021; Accepted 17 June 2021
Available online 24 June 2021

Peterson et al. (2016) study concluded that simple mixing with zero oxygen or sulfidic SGD lowered the oxygen content of bottom waters off South Carolina. A similar mechanism has been suggested as a possible contributor to bottom water hypoxia in the Changjiang (Yangtze) River estuary (Guo et al., 2020). The concepts of "bottom up" versus "top down" controls via nutrient enrichment were first introduced by ecologists to discuss the influence of resource availability and food web actors on ecosystem health (Carpenter et al., 1985). Lapointe (1997) subsequently showed that the bottom-up control of nutrient enrichment from SGD was a causal factor for the development of macroalgal blooms on coral reefs, therefore arguing against the strict control of grazing activity on the development of the bloom. Here, we explore an extension of these concepts by hypothesizing that SGD can exert a bottom-up contribution to coastal hypoxia not just by delivery of zero oxygen waters or bloom-stimulating nutrients, but also by the delivery of reduced species such as ammonium and methane that create an additional oxygen demand in bottom waters.

The Northern Gulf of Mexico hosts the largest hypoxic area in the US coastal waters, and the second largest in the world, with its well-known extensive seasonal hypoxia occurring over the Louisiana-Texas continental shelf to the west of Mississippi River Delta (Rabalais et al., 2002). In that system, the Mississippi and Atchafalaya Rivers, which discharge onto the Louisiana Shelf, supply a large amount of allochthonous nitrogen principally attributable to anthropogenic, agricultural fertilizer use (Donner et al., 2002; Justić et al., 2002) leading to the view of a "top-down", anthropogenically-influenced hypoxic system.

East of the Mississippi River Delta, the Mississippi Bight and Sound also experience seasonal hypoxia (Brunner et al., 2006; Ho et al., 2019; Moshogianis et al., 2013; Rakocinski and Menke, 2016); however, this system, which is offshore a series of barrier islands, is far less studied than the adjacent hypoxic waters to the west of the delta. Hypoxia in the Mississippi Bight was thought to be intermittent since the mid-20th century, based on foraminiferal proxies in sediment cores (Brunner et al., 2006). Nevertheless, a time series conducted at two stations in the Bight between 2008 and 2012 showed regular occurrence of seasonal hypoxia and raised concerns about the function and structure of the macrobenthic community (Moshogianis et al., 2013; Rakocinski and Menke, 2016). The 2008 hypoxic event was the most severe observed during that study period and was suggested to have resulted from enhanced freshwater discharge of nutrient-rich Mississippi River (Rakocinski and Menke, 2016). Dzwonkowski et al. (2018) detailed hypoxia in the Mississippi Bight during summer 2016, pointing out that the region of freshwater influence east of the Mississippi River Delta was as extensive as the better-studied region to the west. However, despite this similarity to the Louisiana Shelf, Sanial et al. (2019) used the stable isotopic composition of water to demonstrate a minimal influence of Mississippi River discharge in the Mississippi Bight as compared with the influence of other more local rivers. As pointed out by Sanial et al. (2019), this is compatible with the regional circulation which most of the year causes Mississippi River discharge to flow west, away from the Mississippi Bight. However, this limited input of nutrient-rich Mississippi River discharge is problematic for discerning of the cause of Bight hypoxia, since the local rivers that dominate the Bight's freshwater supply have much lower nutrient fluxes than the Mississippi River (Dortch et al., 2007; Dunn, 1996).

These observations led us to investigate whether SGD might be involved in the development of hypoxia in the Mississippi Bight. Submarine groundwater discharge is described as any flow of water across the sea floor, and includes circulation of seawater through sediments and discharge of terrestrial freshwater (Burnett et al., 2003). In fact, the circulated seawater component generally dominates over the fresh terrestrial component and thus SGD is often not associated with substantial variation in bottom salinity (Burnett et al., 2003). SGD fluids bypass the estuarine filter that affects river water (Moore and Shaw, 2008), resulting in a hidden pathway for substantial input of materials to the ocean (Moore and Shaw, 2008), including nutrients and metals (Charette and Sholkovitz, 2006), which may have anthropogenic sources such as from excessive agricultural use (Bishop et al., 2015). Note that SGD might further be divided into deeply-sourced SGD with a length scale of meters to kilometers versus pore water exchange ("PEX") with a length scale shorter than meters (e.g., Cai et al., 2014; Rodellas et al., 2017; Santos et al., 2012); we do not make such distinctions in this paper. SGD-derived nutrients can have harmful consequences on the quality of coastal waters by stimulating primary production, leading to coastal eutrophication as well as harmful algal blooms (Paerl, 1997; Slomp and Van Cappellen, 2004), including in the Gulf of Mexico (Hu et al., 2006). A study conducted in Tampa Bay, on the Gulf of Mexico coast of Florida, showed that saline and brackish SGD supplied important quantities of phosphate, dissolved organic nitrogen, and dissolved inorganic nitrogen almost exclusively in reduced forms (Kroeger et al., 2007). This dissolved organic and reduced inorganic nitrogen should create an oxygen demand, representing a potential bottom-up contribution to the development of hypoxia.

In and near the Mississippi Bight, there is other evidence to suggest a need to consider SGD in this study region. For example, Kolker et al. (2013), Krest et al. (1999), and Liefer et al. (2014) all reported evidence of SGD impacts in the central northern Gulf of Mexico. Recently, anoxic SGD inputs were suggested as a mechanism responsible for large fish kills occurring locally in Mobile Bay, Alabama (Montiel et al., 2018), though the oxygen demand of reduced species in the SGD was not described. SGD was also suspected to occur in the western corner of the Mississippi Bight/Sound where episodic hypoxic events take place (Ho et al., 2019). Both the Mississippi River Delta region, and the Mississippi Sound and Bight are known to have buried sandy paleochannels resulting from thousands of years of sea level variations (Greene et al., 2007) that could serve as pathways for groundwater flow (Kolker et al., 2013; Spalt et al., 2018). Furthermore, the uppermost portion of the Louisiana/Mississippi aquifer is composed of different permeable zones that merge with the Mississippi River Valley alluvial aquifer, allowing groundwater flow (McCoy et al., 2007). Likewise, sandy sediments, which can serve as a pathway for the circulated seawater component of SGD, are found distributed through the Bight (Supplementary Fig. S1; Greer et al., 2018; Warner et al., 2010). All of this evidence strengthens the need to investigate the role of SGD in the development of hypoxia in the northern Gulf of Mexico.

2. Materials and methods

2.1. Study area and sampling

The Mississippi Bight is a wide, shallow shelf area to the east of the Mississippi River birdfoot delta. The Bight extends from Mobile Bay to the Chandeleur Islands and has a northern boundary delimited by the barrier islands of the Mississippi Sound (Fig. 1). Despite the proximity of the Mississippi River, $\delta^{18}O$ analysis of river water and seawater (Sanial et al., 2019) reveals that freshwater input to the Bight is usually dominated by local (i.e., Mississippi/Alabama [MS/AL]) river sources, including outflow from Mobile Bay, rather than by the Mississippi River outflow. This is consistent with satellite imagery as well as modeling and drifter studies (Allison et al., 2012; Androulidakis and Kourafalou, 2013; Morey et al., 2003) that show the Mississippi River plume is generally directed south and then west usually with only episodic flow to the east. However, when the river reaches flood stage, the Bonnet Carré Spillway may be opened to relieve pressure on the Mississippi River levees in the New Orleans area. The spillway diverts Mississippi River water eastward, through Lake Pontchartrain, and from there towards the Mississippi Sound and Bight (e.g., Parra et al., 2020).

Four Mississippi Bight sampling campaigns were conducted in 2015–2016 as part of the CONCORDE study of this coastal river-dominated system (Greer et al., 2018). The four cruises occurred in: fall 2015 (Oct 29 – Nov 5), winter 2016 (Feb 10–12), spring 2016 (March 30 – Apr 10), and summer 2016 (July 23–30). The fall, spring,

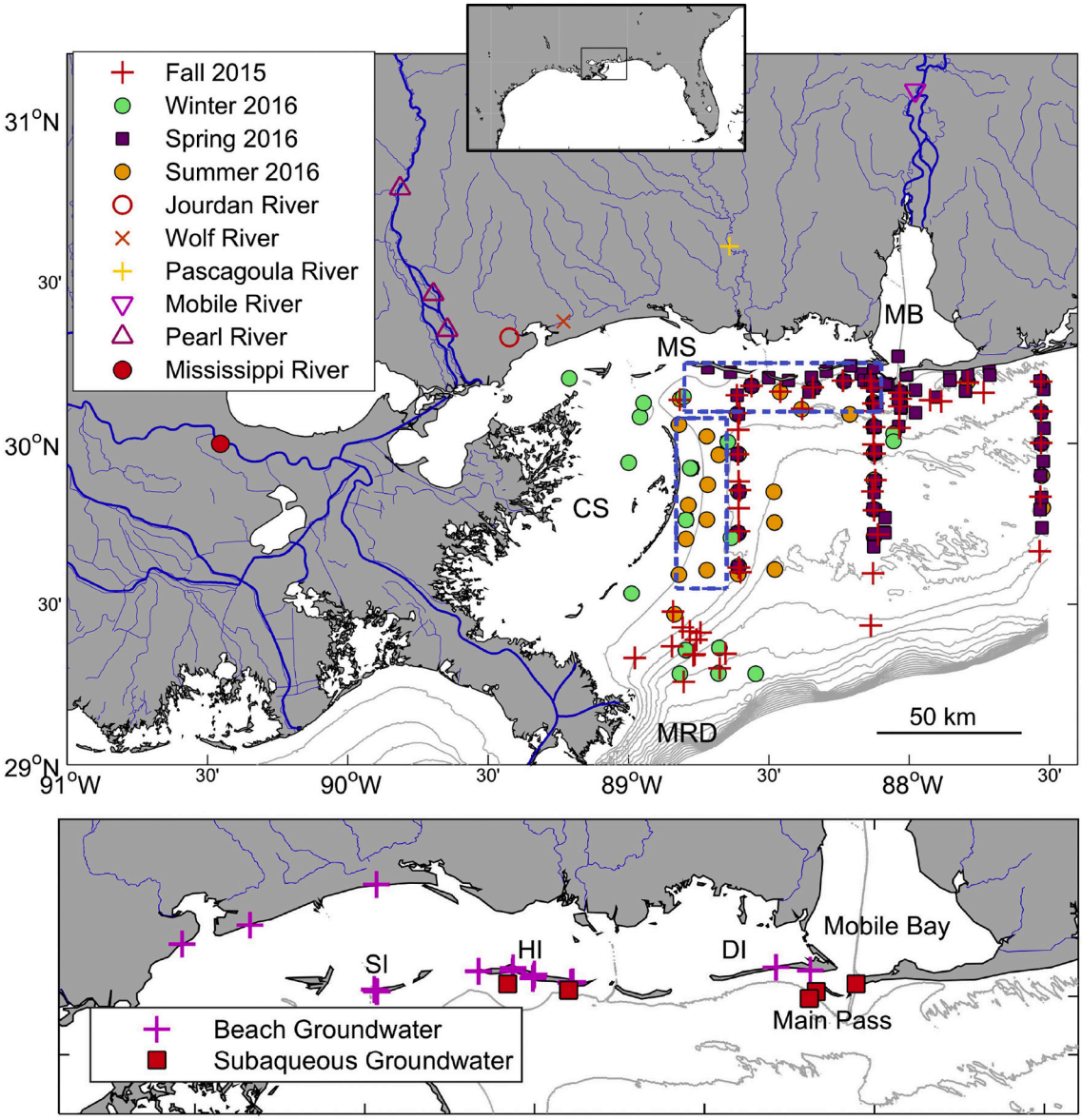

Fig. 1. Sample locations for the four Mississippi Bight field campaigns (Fall 2015, Winter 2016, Spring 2016, Summer 2016) which were part of the CONCORDE study. River sample locations are shown on the top map, while locations of the groundwater samples are shown on the bottom map (representing an expansion on the Mississippi Sound area). Major rivers are shown in thick lines and minor streams are in thin blue lines. The dashed outline highlights the regions near the barrier islands where the strongest SGD influence was observed. The bathymetry is shown in gray with isobaths from 10 to 200 m with contours every 10 m. MB: Mobile Bay. MS: Mississippi Sound. CS: Chandeleur Sound. MRD: Mississippi River Delta. HI: Horn Island. DI: Dauphin Island. SI: Ship Island. (For interpretation of the references to colour in this figure legend, the reader is referred to the web version of this article.)

and summer cruises focused on three north-south sampling corridors. The fall 2015 cruise occurred during a period of low river discharge as well as immediately after remnants of Hurricane Patricia passed through the region. This resulted in increased vertical mixing but also increased flushing of estuarine materials onto the shelf (Dzwonkowski et al., 2017). The winter 2016 cruise was a brief sampling campaign aimed at examining potential impacts on the shelf from the January 2016 opening of the Bonnet Carré Spillway (Parra et al., 2020); the spillway was not open during our other campaigns.

Seawater was collected using acid-cleaned, Teflon-coated, Niskin bottles mounted on a rosette system at surface, mid-, and bottom depth for nutrients (DSi, DIN, TDN, DIP), dissolved trace elements (barium: Ba, manganese: Mn, and molybdenum: Mo), and methane (summer only). Most of the deep samples were in the range 12–20 m; the deepest sample was 37 m. Large volume (~200 L) seawater samples were also collected for radium (Ra) analysis using a hose from a deck-mounted swimming pool pump that was attached to the rosette wire. Because of the cumbersome nature of the large volume samples and their lengthier processing time, Ra samples were collected at only a subset of the stations. Also, while Ra, trace metal, and nutrient samples were collected simultaneously, there was likely a slight difference in depth between samples collected from the pool pump and those collected from the Niskin bottles, which may be relevant considering the shallow, stratified water column in this region. The large volume Ra samples were passed unfiltered through manganese-impregnated acrylic fibers ("Mn fibers") to extract the Ra, rinsed with MQ water, and partially dried (Moore, 1976; Sun and Torgersen, 1998). The Niskin samples were filtered soon after collection through 0.45 μm pore size polyethylene syringe filters using all-polyethylene syringes and stored in polyethylene bottles (Shiller, 2003); all of the filtration materials were acid-washed in a clean lab in advance. Nutrient samples were stored frozen until analysis. Trace metal samples were acidified in a shore-based clean lab to pH < 2 with 6

M ultrapure hydrochloric acid.

For freshwaters, five field trips were conducted to collect samples from the Mississippi, Jourdan, Wolf, Pascagoula, Pearl, and Mobile Rivers between October 2015 and June 2016 (Fig. 1). Approximately 20 L samples were collected for radium analysis, as well as an additional 50 mL for measurements of Ba and nutrients. The river samples were filtered/processed similarly to the seawater samples. River waters were also collected to determine the suspended particulate matter (SPM) concentrations in these rivers between April and March 2018 to constrain the flux due to desorbable fractions of species (such as radium). The SPM concentration was measured twice in the Pearl and Wolf Rivers from samples collected in two different field trips, and once in the other rivers. Approximately 500 mL were filtered through 0.45 μm pore size filters. The filters were then dried and weighed to deduce the SPM concentration.

Fifty-nine groundwater samples were collected between April 2016 and March 2017 on the MS/AL barrier islands (Horn Island, Ship Island, and Dauphin Island) and on mainland beaches (Mainland) (Fig. 1). The groundwater samples were collected between the beach face and 2 m deep using Push Point samplers (MHE Products; e.g., Zimmerman et al., 2005) and a peristaltic pump. These samples ranged in salinity from 0 to 33. During the sampling trip on Horn Island, we found and sampled two ponds with brackish waters, salinities of 28.5 and 14.4, further highlighting the presence of groundwater percolating to the surface. Additionally, a few subaqueous groundwater samples were collected south of Horn and Dauphin Islands (Fig. 1) by divers using a modified Push Point sampler. The water depth at these locations was 9–11 m. Obtaining water samples from Mississippi Bight sediments in sufficient quantity for Ra determination was problematic due to the muddy to fine sand nature of the Bight sediments (Supplementary Fig. S1). Ra activities could only be measured in one sample with a larger volume; Ba concentrations were measured in all samples. The samples from south of Dauphin Island were collected in March 2017 and had salinities of 32–33. The samples from south of Horn Island were collected in June 2019 and had salinities of 24.6 and 30.9. Processing of groundwater samples proceeded similarly to the processing of river and seawater samples.

2.2. Sample analysis

Trace metal and nutrient concentrations, as well as ^{223}Ra, ^{224}Ra, ^{226}Ra, and ^{228}Ra activities were measured in seawater, groundwater, and freshwater. The ^{224}Ra and ^{223}Ra activities were determined using a RaDeCC system (Moore, 2008; Moore and Arnold, 1996) as soon as possible after collection. The samples were run again two weeks and two months later to account for the supported ^{224}Ra and ^{223}Ra, respectively. The Mn fibers were then leached with HCl and hydroxylamine hydrochloride to remove the Ra from the fibers. The Ra was coprecipitated with $BaSO_4$ and the precipitants were transferred into small vials and aged for 3 weeks to allow the ingrowth of ^{222}Rn (Moore, 1984). The samples were then measured on gamma spectrometers at the University of South Carolina to determine the ^{226}Ra and ^{228}Ra activities.

Nutrient analyses were performed at the Dauphin Island Sea Lab. Dissolved inorganic nitrogen (NO_x and NH_4^+) and phosphorus (DIP) were quantified colorimetrically using a Skalar autoanalyzer (Macintyre et al., 2011). Total dissolved nitrogen (TDN) was also determined colorimetrically as nitrate after oxidation (Solórzano and Sharp, 1980). Dissolved silicic acid (DSi) was analyzed using a manual colorimetric method (Brzezinski and Nelson, 1995). The dissolved organic nitrogen (DON) concentrations were estimated by subtracting the dissolved inorganic nitrogen (DIN) from the total dissolved nitrogen (TDN).

Dissolved Ba and Mo concentrations were measured on a high resolution inductively coupled plasma mass spectrometer (HR-ICP-MS) and were determined using an isotope dilution method (Ho et al., 2019; Joung and Shiller, 2013). The Mn concentrations were analyzed by HR-ICP-MS either by dilution with external standards calibration (for higher concentrations) or by using the Magnesium-Induced Co-precipitation method (MagIC) method with Fe and Cu used as internal standards (Shim et al., 2012).

Dissolved methane was determined at sea using cavity ringdown spectroscopy (Picarro G2301) following the method of Roberts and Shiller (2015). Dissolved oxygen concentrations were taken from the CTD data as calibrated with discrete samples measured by Winkler titration. Salinity data were obtained from the CTD. However, because of sharp surface water salinity gradients and placement of the CTD salinity sensor below the Niskin bottles, the surface water salinity was derived from dissolved molybdenum concentrations in the Niskin samples (Sanial et al., 2019). Similarly, the salinity for the two deep groundwater samples collected by the divers was calculated from the molybdenum concentrations.

All data produced in these surveys can be found online through the Gulf of Mexico Research Initiative Information & Data Cooperative (https://data.gulfresearchinitiative.org/; see also Supplementary Table S1).

2.3. Estimation of desorbable radium from river suspended particulate matter

Experiments were set up to estimate the desorbable fraction of radium in order to better constrain the radium river flux. The river SPM was the highest in Pearl River (136 mg L^{-1}), followed by Mobile (37 mg L^{-1}), Pascagoula (34 mg L^{-1}), Jourdan (24 mg L^{-1}), and Wolf (18 mg L^{-1}) Rivers. The weighted average SPM was thus estimated at 52 mg L^{-1}. Desorption experiments were therefore conducted on Pearl River water, which has the highest SPM load. Two freshwater samples were collected, filtered in the field through a 0.45 μm capsule filter, followed by Mn fiber for Ra extraction. Two additional large volume freshwater samples were collected, brought back to the lab where the salinity was artificially increased to 29 to ensure desorption from particles was complete. The water was recirculated for a minimum of 24 h using submersible pumps, and subsequently filtered through a 0.45 μm capsule filter, followed by Mn fiber extraction. Considering the SPM content in that sample of 167 mg L^{-1}, the desorbed Ra from SPM was estimated at 0.72 dpm g^{-1} for ^{228}Ra and 0.97 dpm g^{-1} for ^{226}Ra, leading to a desorbable Ra fraction of 38% for ^{228}Ra and 54% for ^{226}Ra. This desorbable fraction is within the range of expected ^{228}Ra desorption rate from river SPM (e.g., 0.5 ± 0.4 dpm g^{-1} of suspended particles; Rodellas et al., 2015a, 2015b) as well as experiments conducted in the Mississippi – Atchafalaya River plumes (Krest et al., 1999). The percentage of desorbable ^{226}Ra from our experiments slightly exceeded the value found by Krest et al. (1999). We estimated that the desorbable fraction from river-borne SPM accounts for 22% of ^{228}Ra and 32% of ^{226}Ra relative to the total stream source. These are included in our riverine supply values. Unfortunately, the duration of the experiment was too long to obtain meaningful short-lived Ra desorption data, though these can be estimated by assuming similar partition coefficients among the Ra isotopes.

3. Results and discussion

3.1. Chemical composition of shallow groundwater and river water

The salinity of groundwater sampled on the MS/AL barrier islands and on mainland Mississippi beaches (Fig. 1) ranged from 0 to 33.3 (mean/median = 13.7/12.9). The activities of the Ra quartet (reported as dpm 100 L^{-1}) ranged from below detection to maxima of: ^{223}Ra: 65, ^{224}Ra: 1150, ^{226}Ra: 78, and ^{228}Ra: 647. The mean/median values of the quartet were ^{223}Ra: 11/8, ^{224}Ra: 181/121, ^{226}Ra: 19/14, and ^{228}Ra: 72/83. (Note that values below detection were counted as '0' in the averages.) Dissolved Ba concentrations ranged from 3 to 1650 nM (230/240 nM mean/median) and the DSi concentrations ranged from 8 μM to 573 μM (148/56 μM mean/median). The Ba concentrations from the subaqueous groundwater samples collected offshore of the barrier islands (174–530 nM) were within the range of the shallow beach groundwater

samples. Only the eastern Horn Island subaqueous groundwater sample had enough volume for Ra determination: ^{223}Ra: 20 dpm 100 L^{-1}, ^{224}Ra: 330 dpm 100 L^{-1}, ^{226}Ra: 62 dpm 100 L^{-1}, ^{228}Ra: 242 dpm 100 L^{-1}, which are similar to the Ra activities and activity ratios of groundwater from mainland and barrier island beaches. These limited subaqueous samples suggest that our approach of focusing on more readily obtainable beach/barrier island groundwater samples likely provided a reasonable estimate of the composition of regional SGD. Indeed, brackish ponds and an artesian well are present on Horn Island, further suggesting a regional connection between fresh terrestrial groundwater, circulated seawater, and SGD.

Dissolved inorganic phosphate and DIN concentrations were also elevated in groundwater, with DIP values up to 26 μM and DIN up to 525 μM. Most of the inorganic nitrogen was in the reduced form, resulting in an NH_4^+/DIN ratio above 0.5 in 80% of the samples. A significant amount of nitrogen was also found as dissolved organic nitrogen, with DON concentrations up to 147 μM and an average of 32 ± 32 μM. Approximately half of the groundwater samples displayed DON/TDN ratios above 0.5, suggesting that groundwater could also supply Mississippi Bight bottom waters with significant fixed N as DON. The DIN:DIP ratios in groundwater ranged from 0.1 to 51 with an average of 12, which indicates a large variability and an average value slightly in excess of phosphate relative to the global phytoplankton atomic ratio uptake. High dissolved methane concentrations (including a number of samples with concentrations in the μM range) were also measured in samples collected on MS/AL barrier islands, consistent with highly reducing groundwater.

In order to estimate the impact of SGD on Mississippi Bight chemical composition (Section 3.4 and following), we needed to select reasonable estimates of the SGD endmember entering these relatively shallow bottom waters. This is problematic due to the spatial and temporal variability of SGD composition. We focused on the high salinity SGD samples, since Bight bottom waters did not show a significant freshwater signature (see next section). Constituent variability in our high salinity samples was often ~100% (RSD), which suggests that the SGD impacts we estimate are probably off by less than a factor of two; this still allows us to address the basic question of whether or not SGD is a significant factor in Bight biogeochemistry. As will be shown below, our endmember estimates of differing constituents lead to similar conclusions, lending confidence to our approach. Where constituent trends with salinity were highly scattered, we calculated the mean and median concentrations of SGD samples with $S > 26$ ($n \sim 10$, depending on constituent) and used an intermediate value as the endmember estimate. Where the constituent concentration varied with salinity (Ba and Ra), we used as the endmember the constituent-salinity trend value at $S = 34.7$, i.e., the mean Bight bottom salinity observed during spring and summer. This approach led us to adopt the following endmember concentrations: Ba = 331 nM; ^{223}Ra = 17.7 dpm 100 L^{-1}; ^{224}Ra = 296 dpm 100 L^{-1}; ^{226}Ra = 29.8 dpm 100 L^{-1}; ^{228}Ra = 126 dpm 100 L^{-1}; DSi = 144 μM; DIN = 36.7 μM; DON = 40.5 μM; NH_4^+ = 26.5 μM; DIP = 3.6 μM; CH_4 = 309 nM.

We estimated the relative contribution of the local MS/AL rivers based on the river monitoring data from the USGS Current Conditions for the Nation (https://waterdata.usgs.gov/nwis/uv?). The Mobile River contributes the most to the freshwater discharge (~ 56%), followed by Pearl and Pascagoula (~ 17% each), and Jourdan and Wolf (~ 5% each). The average concentrations of chemical elements from the five trips to each river were then weighted with their relative contribution to the freshwater discharge to the Mississippi Bight. The Ra activities in river water were well below groundwater concentrations, with weighted average of: ^{223}Ra: 0.3 ± 0.1 dpm 100 L^{-1}, ^{224}Ra: 12 ± 4 dpm 100 L^{-1}, ^{226}Ra: 11 ± 1 dpm 100 L^{-1}, ^{228}Ra: 13 ± 4 dpm 100 L^{-1}. Ba and DSi concentrations were estimated at 223 ± 17 nM and 40 ± 20 μM. The average nutrient contents of the local MS/AL rivers were DIN: 15 ± 4 μM, DON: 30 ± 3 μM, DIP: 0.5 ± 0.1 μM. These values are overall lower than in the Mississippi River (^{223}Ra: 0.3 dpm 100 L^{-1}, ^{224}Ra: 24 dpm 100 L^{-1}, ^{226}Ra: 16 dpm 100 L^{-1}, ^{228}Ra: 24 dpm 100 L^{-1}, Ba: 440 nM, DSi: 94 μM, DIN: 126 μM, DON: 122 μM, DIP: 2.4 μM) (Shiller et al., 2019).

3.2. Chemical distributions in the Mississippi Bight: relationships with salinity, location, and time

Surface waters showed the expected temporal/spatial salinity trends (Supplementary Fig. S2). That is, surface water salinity was generally high during low river discharge (fall) and low during high river discharge (spring) with lower values closer to the coast (i.e., northward and westward) than offshore. In general, the eastern sampling corridor showed the highest salinities, consistent both with the major freshwater sources being Mobile Bay and the Mississippi River Delta as well as with the usual westward flow in the Bight (e.g., Dzwonkowski et al., 2011; Walker et al., 2005). The limited spatial coverage in winter prevents broad conclusions for that survey, though surface salinities were rather variable, likely due to unusually high winter discharge and the flood control diversion of some Mississippi River outflow into Lake Pontchartrain (e.g., Sanial et al., 2019; Parra et al., 2020). Interestingly, the lowest surface salinity in the eastern corridor occurred during summer which, while still relatively high compared to the rest of the Bight, is the time of year when southwest winds can drive surface water flow eastward (Dzwonkowski et al., 2018 and references therein). In contrast to the occasional significant freshening of the surface waters, bottom waters in the Bight are consistently saline with most samples having salinities of 34 or higher (Supplementary Fig. S2). Thus, despite this being a river-dominated system, bottom waters generally have open Gulf salinities year-round.

The temperature in spring (Supplementary Fig. S3) was relatively homogeneous throughout the water column and also spatially in the Mississippi Bight. In summer, the water column generally warmed, with a difference of temperature of approximately 5 °C between surface and bottom waters. The density profiles suggest that the water column was generally stratified both in spring and summer (Supplementary Fig. S3). However, the spring stratification was mainly caused by low surface salinity whereas the summer stratification was mostly driven by the warm surface layer.

Hypoxic bottom waters were not observed in fall or winter (Fig. 2). In spring 2016, only a few samples collected in bottom waters near Main Pass of Mobile Bay were hypoxic. Nonetheless, CTD profiles showed several stations with near-hypoxic bottom water (Supplementary Fig. S3). In the summer survey, however, the bottom water DO was much lower, with concentrations down to 1 μM within a relatively large hypoxic area east of the Chandeleur Islands (Fig. 2). Time series of DO concentrations from three moorings in the Mississippi Bight in summer 2016 showed substantial temporal variability of DO concentrations with several episodic hypoxic events; the most frequent and intense ones were found near the northwestern corner of the Mississippi Bight (see Fig. 6 in Dzwonkowski et al., 2018). Dzwonkowski et al. (2018) presented mooring data in the northwest corner of the Mississippi Bight demonstrating bottom waters were hypoxic for approximately 6 days (July 19–25) prior to the summer 2016 cruise. We note that those moorings were located outside of the hypoxic region shown in our data, suggesting that the hypoxic zone is likely larger than revealed by our survey.

The distribution of dissolved Ba versus salinity (Figs. 3 & 4) in Mississippi Bight surface waters (yellow symbols) shows Ba concentrations generally falling on mixing lines (red lines) extending from typical offshore concentrations (i.e., 53 nM at salinity 36.4; Joung and Shiller, 2013) to effective river concentrations of Ba ranging from 225 to 450 nM in spring to 250–900 nM in summer. The lower values are compatible with local river dissolved Ba concentrations (220 ± 40 nM); the 450 nM concentration is similar to Mississippi River Ba concentrations (our data and Shiller, 1997); in contrast, the highest effective endmember Ba concentration is somewhat higher than the highest effective endmember

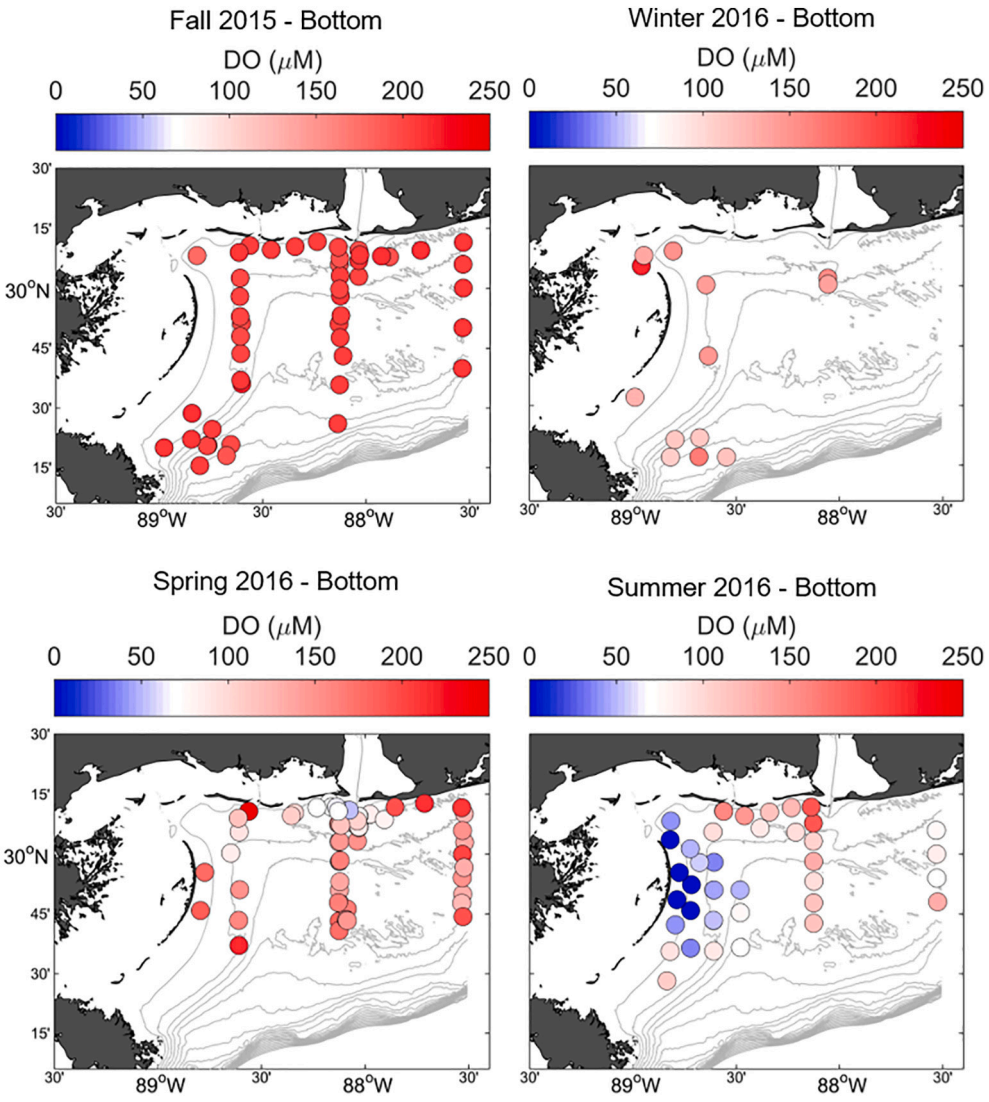

Fig. 2. Dissolved oxygen concentration (DO) in Mississippi Bight bottom waters (<2 m above the seafloor). Blue colour shows DO concentrations near or below hypoxic level (≤63 μM). Bathymetry is shown in gray with isobaths from 10 to 200 m, with contours every 10 m. (For interpretation of the references to colour in this figure legend, the reader is referred to the web version of this article.)

observed by Joung and Shiller (2014). In general, then, the surface water Ba distribution conforms to expectations for a mixing environment with two rather different types of river waters and with occasional additional input, possibly from the bottom (Joung and Shiller, 2014). Bottom waters, however, all fall above these surface water mixing relationships (Figs. 3 and 4, blue symbols), indicating that another Ba source is required besides offshore waters and fluvial contributions.

In the Mississippi Bight bottom waters, dissolved barium (Ba; Figs. 5 and 6) shows a roughly inverse relationship, spatially and temporally, to DO. In spring and summer 2016, these bottom water Ba concentrations were high relative to open Gulf waters (50–55 nM; Joung and Shiller, 2013). As noted above, since the bottom waters were salty, this enrichment is not likely due to admixture of river water (Joung and Shiller, 2014) and the enrichment is greater than can be accounted for by upwelling of off-shelf waters (Joung and Shiller, 2013). Dissolution of Ba-rich drilling muds is also unlikely to account for this (Joung and Shiller, 2014) and diffusive fluxes from the sediments are probably too low by an order of magnitude (Ho et al., 2019; McManus et al., 1998). However, salty groundwater is generally enriched in Ba (Gonneea et al., 2013), with concentrations that can reach an order of magnitude greater than in rivers. Indeed, the SGD Ba flux to coastal/estuarine regions can exceed the riverine inputs (e.g., Southeastern USA: Duncan and Shaw, 2003; Shaw et al., 1998). Thus, the high Ba concentrations in salty bottom waters of the Mississippi Bight are a likely indicator of SGD. High dissolved Ba was also observed in hypoxic bottom waters on the Louisiana Shelf, with SGD being a possible source there, too (Joung and Shiller, 2014). Nonetheless, biological Ba removal from surface waters and remineralization in bottom waters cannot be discounted as a possible source for bottom water Ba enrichment. We further address this possibility below.

For fall 2015, the dissolved Ba in both surface and bottom waters plotted on the same trend with salinity (Supplementary Fig. S4), consistent with storm-induced mixing of the water column. Interestingly, the bottom waters in fall with salinities greater than 35 still showed dissolved Ba concentrations of ~59 nM, i.e., slightly higher than shallow open Gulf waters (Joung and Shiller, 2013). Nonetheless, given that bottom hypoxia as well as distinct Ba enrichment were only observed during spring and summer, we confine further discussion to just those two surveys pertinent to our hypothesis of a connection between hypoxia and SGD.

Similar to Ba, the spring/summer DSi-salinity plots (Figs. 3 & 4) reveal the Bight bottom waters to be significantly enriched in DSi relative to either surface waters or what would be expected from mixing of coastal seawater and river water. The bottom excesses of DSi (relative to

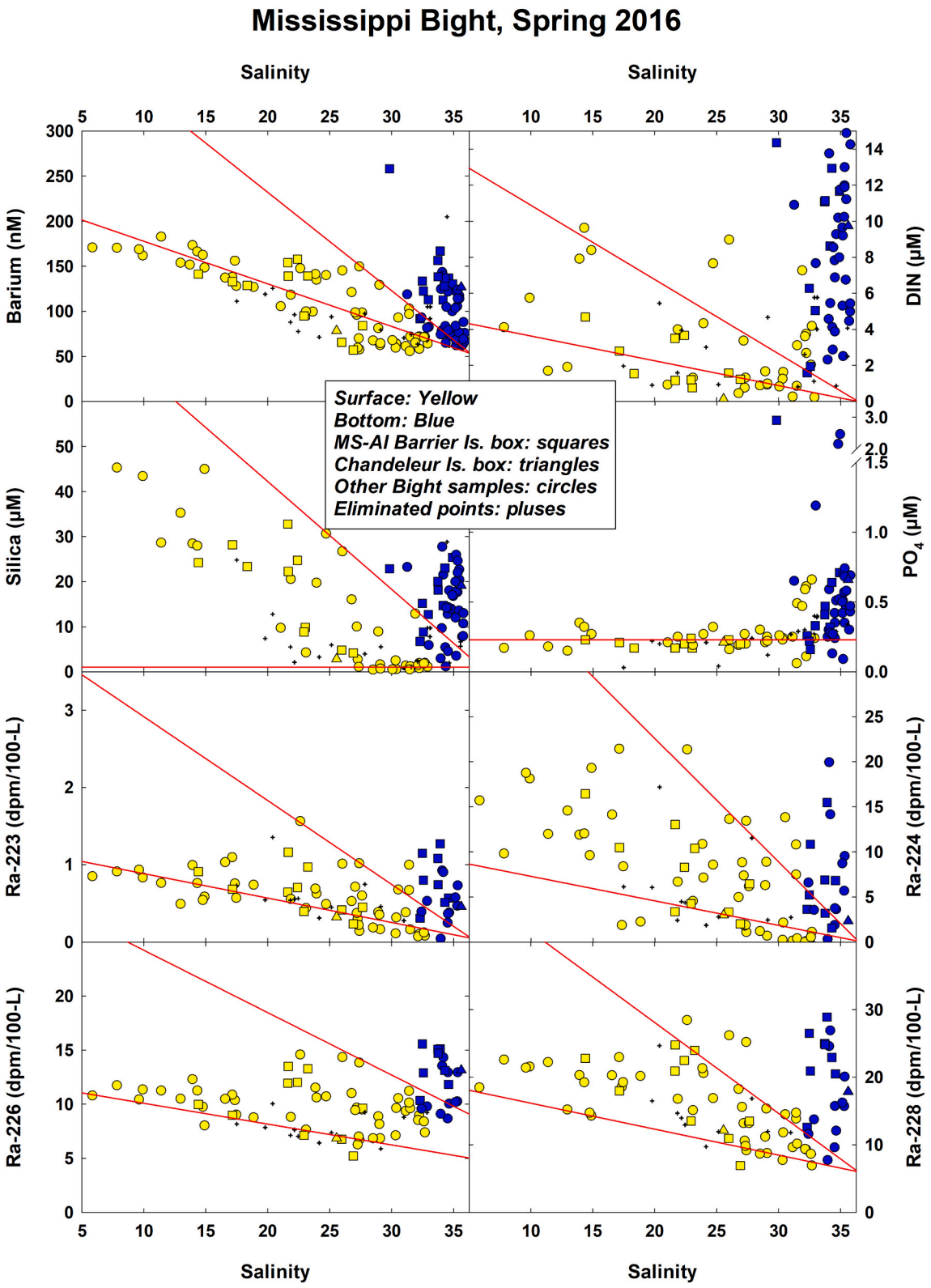

Fig. 3. Dissolved barium (Ba), dissolved inorganic nitrogen (DIN), dissolved silicic acid (DSi), dissolved inorganic phosphorus (DIP) concentrations, and Ra activities (^{223}Ra, ^{224}Ra, ^{228}Ra, ^{226}Ra) as a function of salinity in Mississippi Bight surface (yellow) and bottom (blue) waters in spring 2016. Extrapolations of surface concentration versus salinity to zero salinity are shown in red, and represent trends to the high and low estimates of "effective" river concentrations (C*; see also Supplementary Table S1). (For interpretation of the references to colour in this figure legend, the reader is referred to the web version of this article.)

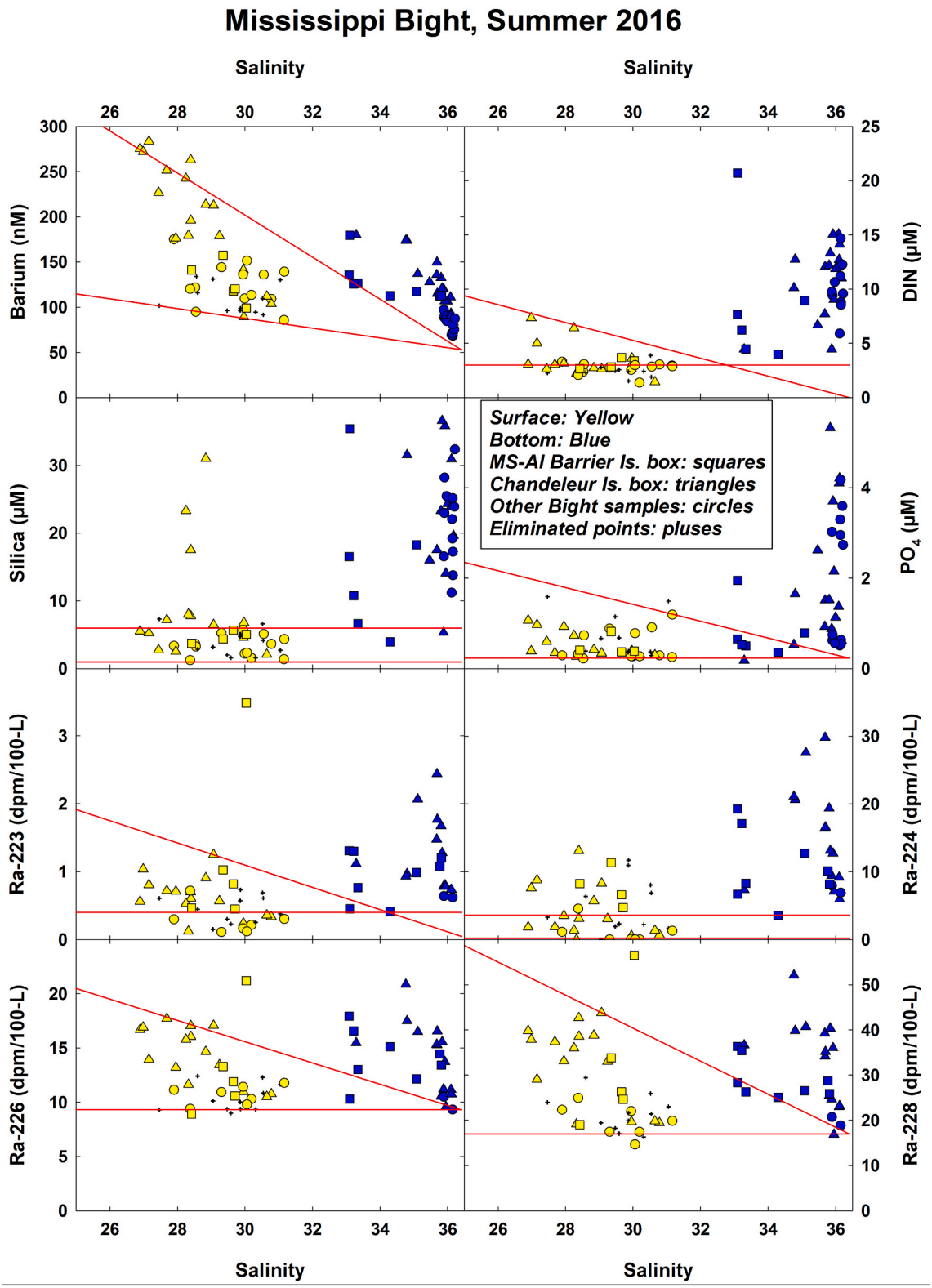

Fig. 4. Dissolved barium (Ba), dissolved inorganic nitrogen (DIN), dissolved silicic acid (DSi), dissolved inorganic phosphorus (DIP) concentrations, and Ra activities (^{223}Ra, ^{224}Ra, ^{228}Ra, ^{226}Ra) as a function of salinity in Mississippi Bight surface (yellow) and bottom (blue) waters in summer 2016. Extrapolations of surface concentration versus salinity to zero salinity are shown in red, and represent trends to high and low estimates of "effective" river concentrations (C*; see also Supplementary Table S1). (For interpretation of the references to colour in this figure legend, the reader is referred to the web version of this article.)

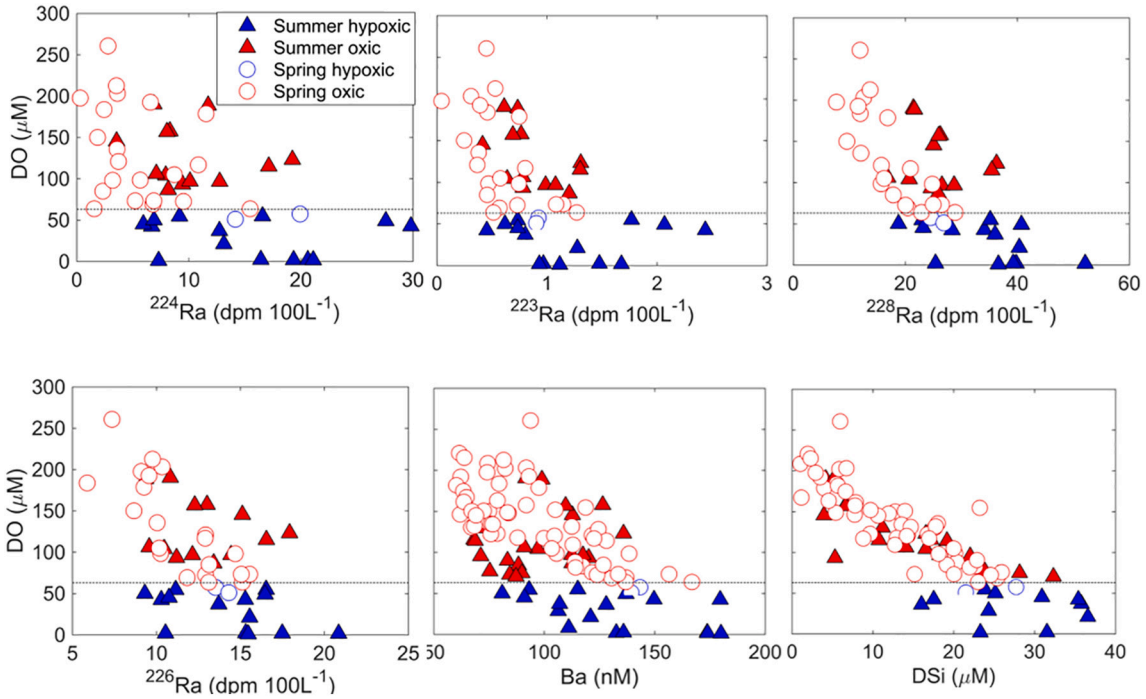

Fig. 5. Dissolved oxygen (DO) versus ^{224}Ra, ^{223}Ra, ^{228}Ra, ^{226}Ra activities, barium (Ba), and silicic acid (DSi) concentrations in Mississippi Bight bottom waters during spring (circles) and summer (triangles). Blue symbols indicate samples below the hypoxia limit of 63 μM DO (also indicated by the horizontal line). (For interpretation of the references to colour in this figure legend, the reader is referred to the web version of this article.)

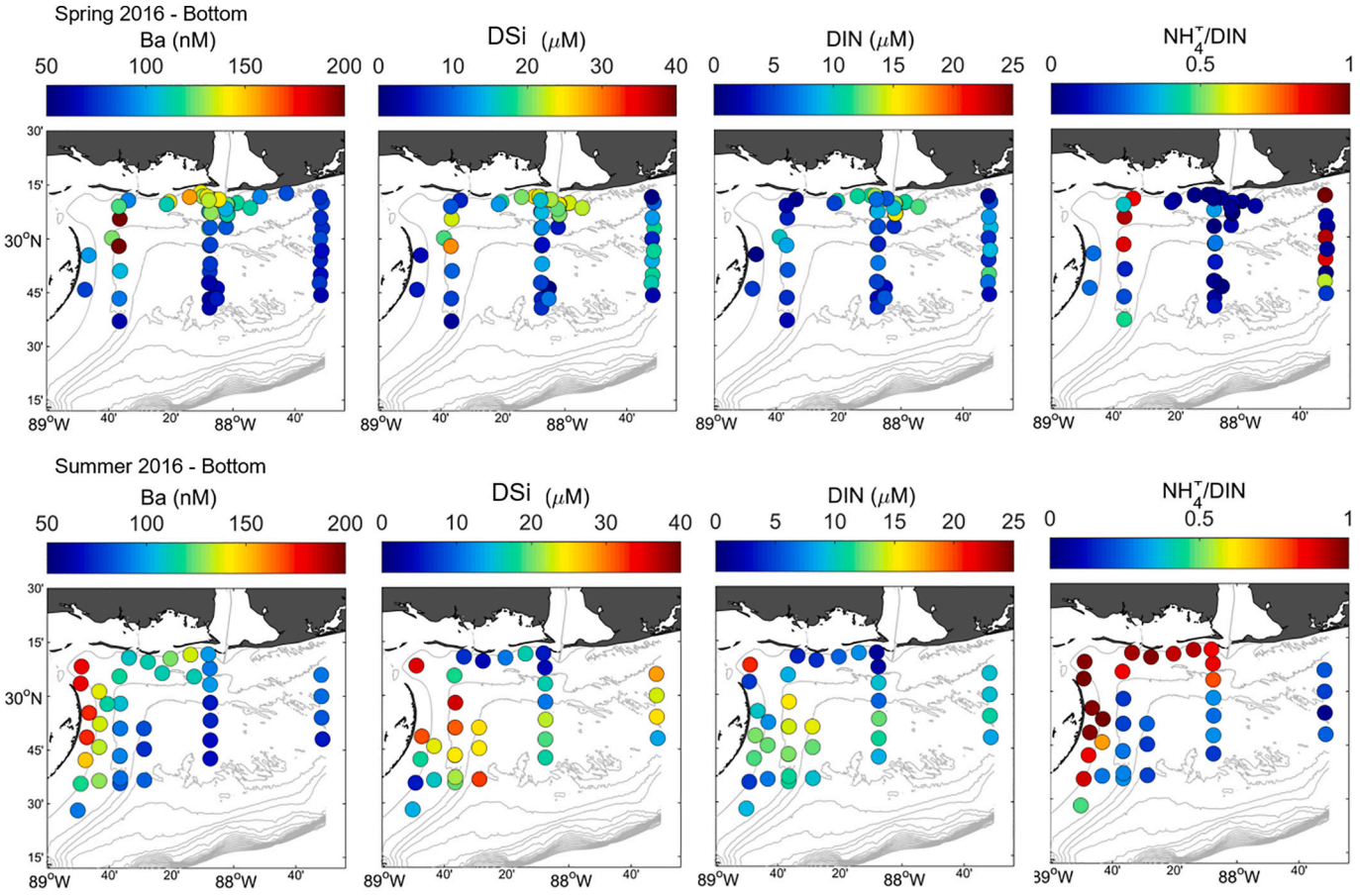

Fig. 6. Dissolved barium (Ba), silicic acid (DSi), and inorganic nitrogen (DIN = NO_x + NH_4) concentrations as well as the ammonium to DIN ratios (NH_4/DIN) in Mississippi Bight bottom waters for spring (top) and summer (bottom) 2016. Bathymetry is shown in gray with isobaths from 10 to 200 m; contours every 10 m.

mixing) are mainly above 10 μM and up to ~30 μM excess DSi. The Bight bottom water DSi distribution displayed a spatial/temporal pattern similar to DO and Ba (Figs. 5 and 6). We note that the bottom DSi concentrations were especially high east of the Chandeleur Islands in the hypoxic regions. As suggested above for Ba, an alternative to SGD input of DSi is a more conventional 'top-down' process whereby DSi is removed biologically from surface waters and subsequently remineralized in bottom waters to give rise to our observed bottom water excess. Indeed, the very low surface water DSi at high salinities implies surface biological removal. We do observe that surface water chlorophyll-a (as a proxy for biological removal) tends to be highest in spring and summer in similar locations where there is low bottom water DO and high bottom water Ba and DSi (Supplementary Fig. S5). So, there is little doubt that conventional top-down biogeochemical cycling is likely important in our study region. But we also note that the ratio of excess Ba to DSi in spring and summer Bight bottom waters is typically about 3 mmol/mol. This is above the Ba/DSi range of 0.017–1.4 mmol/mol reported for bulk plankton (Collier and Edmond, 1984) (Collier and Edmond, 1984). Thus, there is still the need for at least an additional Ba source.

The spatial distribution of dissolved inorganic nitrogen (DIN) in Mississippi Bight bottom waters was also very similar to the Ba, DSi and DO distributions (Fig. 6). Bight bottom waters were significantly enriched in DIN relative to potential contributions from the mixing of river water and offshore waters (Figs. 3 & 4). Furthermore, DIN-enriched hypoxic waters tended to have high NH_4^+/DIN ratios (Fig. 6), suggestive of reduced inputs. The similarities between the Ba, DO, DSi, and DIN distributions in time and space thus suggest a common mechanism driving the chemistry of Mississippi Bight bottom waters.

Dissolved organic nitrogen (DON) was also prevalent in significant concentrations in spring/summer Bight bottom waters, though spring concentrations tended to be higher than summer (Fig. 7). DON was the main form of the total dissolved nitrogen (TDN) in spring as shown by the high DON/TDN ratios; and even in summer DON still could be the major fraction of TDN. At first glance, the bottom DON distribution appears to differ from the other bottom chemical distributions. However, we observed significant ($p < 0.001$) positive correlation between the DON/TDN ratio and DO, and a negative correlation between DON/TDN and DSi. This could simply reflect more efficient remineralization of DON to DIN in the presence of DO.

Interestingly, DSi correlated strongly with TDN (Supplementary Fig. S6) as well as with DIN in bottom waters. Given that dissolved N and Si are derived from different phases (i.e., organic matter vs. biogenic silica) and with organic-N remineralization pathways affected by DO availability, this is surprising and suggests a common source other than remineralization of sinking biological materials for the bottom water enrichments of these two nutrients.

Dissolved phosphate (DIP) concentrations were low and uniform in spring bottom waters, with a maximum value of 0.74 μM (Fig. 7). Bight bottom waters were significantly enriched in DIP relative to potential contributions from the mixing of river water and offshore waters (Figs. 3 & 4). The DIP concentrations were generally much higher in summer bottom waters with concentrations up to 5.3 μM. While there was a rough correspondence between the spatial distribution of DIP and DIN, the correlation was somewhat scattered (Supplementary Fig. S5), with the lower DIP samples (DIP <0.75 μM) showing a Redfield DIN/DIP ratio of 16 while the higher DIP samples (>1 μM) show large increases in DIP with only small changes in DIN. Indeed, the relationship between DIP and DO seemed to show a maximum in DIP around DO

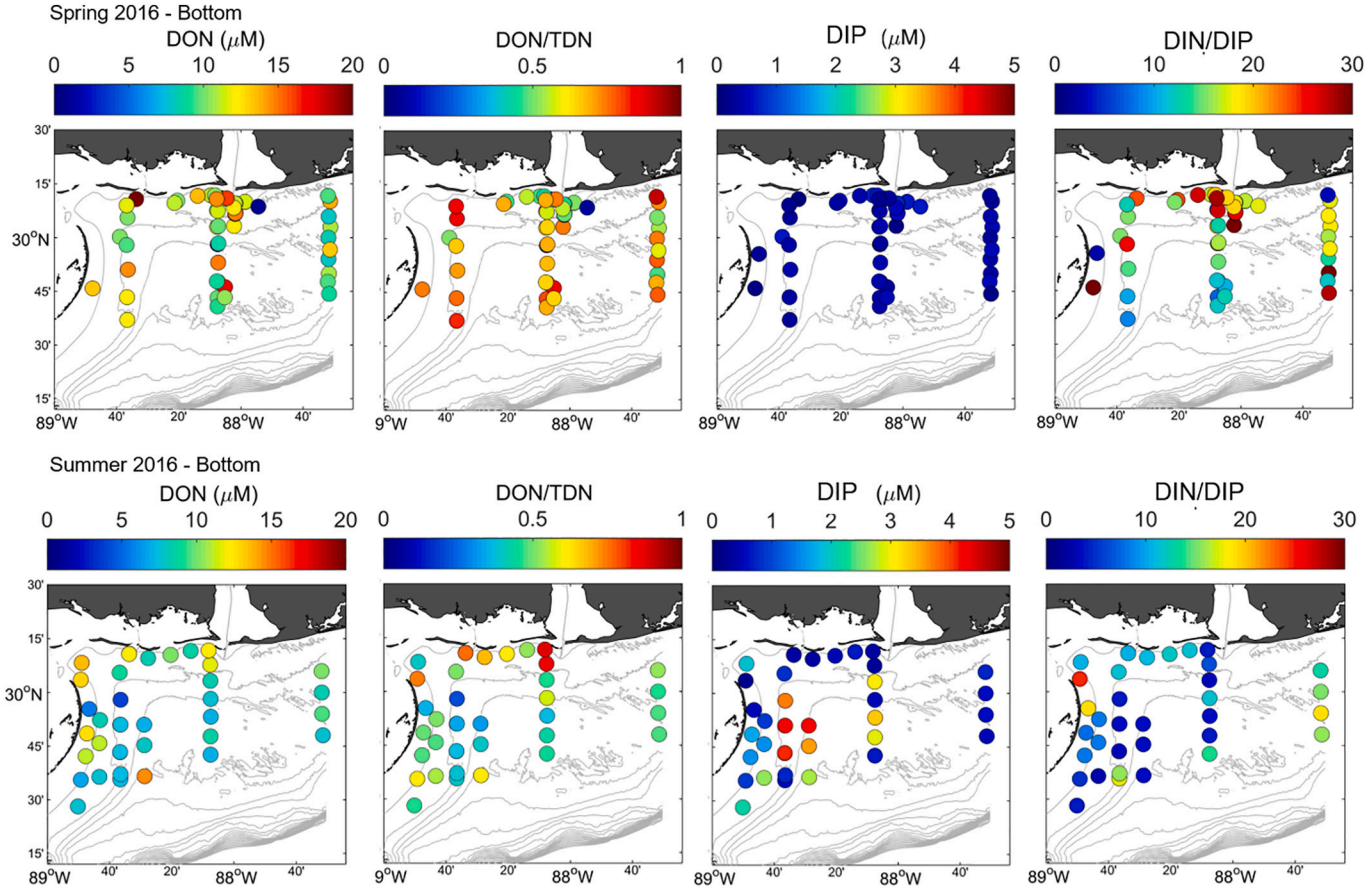

Fig. 7. Dissolved organic nitrogen (DON), DON to total dissolved nitrogen (TDN = DIN + DON) ratios, dissolved inorganic phosphorus (DIP) concentrations, and DIN/DIP ratios in Mississippi Bight bottom waters for spring (top) and summer (bottom) 2016. The bathymetry is shown in gray with isobaths from 10 m to 200 m; contours every 10 m.

concentrations of 50 μM (Supplementary Fig. S6). However, full elucidation of phosphorus cycling in our system is beyond the scope of the present discussion.

Dissolved methane (CH_4) was only determined during the summer survey. Here again, bottom water concentrations were much higher than surface water concentrations and the highest bottom water concentrations occurred east of the Chandeleur Islands, where low DO was also observed (Fig. 8). It seems unlikely that the water column itself was so reducing that these bottom water CH_4 enrichments were generated within the water column; rather, this is indicative of a sedimentary source.

In summary, we observe bottom water enrichments of dissolved Ba, CH_4, and nutrients along with oxygen depletion, co-occurring both spatially and temporally. Our SGD samples indicate that the regional SGD is enriched in these materials. There are also sandy sediments and buried paleo-channels that can serve as conduits for both terrestrial and circulated seawater components of SGD (Greene et al., 2007; Kolker et al., 2013; Spalt et al., 2018). While this supports our hypothesis of a "bottom up" linkage between SGD and hypoxia, nonetheless there are other possible explanations for our observations. The "coincidence" explanation is that water column stratification simultaneously limits re oxygenation of bottom waters and also allows for trapping and build-up of bottom-input Ba, CH_4, and nutrients. Furthermore, the bottom input of nutrients could result from remineralization of organic matter settling into the bottom waters from the surface. In contrast, a "bottom-up" explanation is that SGD delivers Ba- and NH_4^+-enriched anoxic waters that drive the bottom waters to hypoxic conditions through the oxygen demand of the SGD-derived reduced species. These alternatives need not be mutually exclusive.

3.3. Radium isotope distributions in the Mississippi Bight

Because SGD often emanates over broad spatial scales in shelf environments rather than coming from a point source and because it can be spatially and temporally variable, its flux is difficult to quantify. However, the use of radium (Ra) isotopes is a well-established means for providing local and regional scale estimates of SGD (Charette et al., 2001; Moore, 2003). Radium is naturally produced by the constant decay of thorium in sediments; because Ra is mobile with respect to its thorium parent in salty waters, it enters the pore/ground waters. Radium is thus often enriched by several orders of magnitude in groundwater relative to surface waters (Moore, 2003). There are four Ra isotopes with half-lives ranging from 3.66 days (^{224}Ra) to 11.4 days (^{223}Ra) to 5.75 years (^{228}Ra) to 1600 years (^{226}Ra), which provide

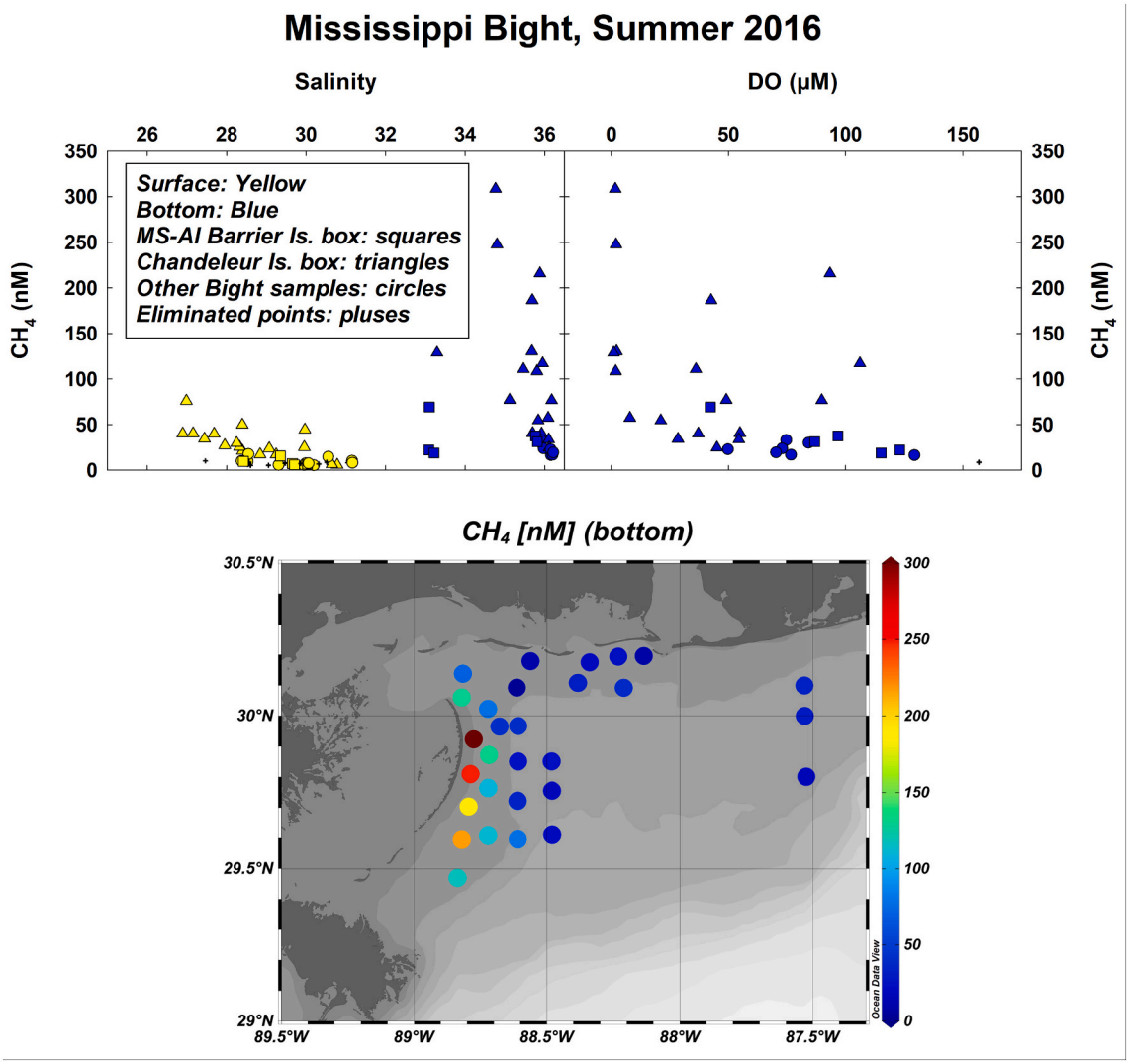

Fig. 8. Methane (CH_4) concentrations measured in surface and bottom Mississippi Bight waters in summer 2016. The scatter plots show CH_4 as a function of salinity and dissolved oxygen (DO). The map shows the spatial distribution of CH_4 in Mississippi Bight bottom waters. The bathymetry is shown in gray with isobaths from 10 m to 200 m; contours every 10 m.

powerful constraints to evaluate the flow rates and chemical fluxes associated with SGD (e.g., nutrients, reduced substances, trace elements).

The ^{226}Ra and ^{228}Ra activities measured in the Mississippi Bight bottom waters (Fig. 9) were above levels previously reported for open Gulf of Mexico surface seawater (Boyle et al., 1984; Reid et al., 1979). Likewise, bottom water activities of short-lived ^{223}Ra and ^{224}Ra (Fig. 9) tended to be higher than high salinity surface water samples off the Louisiana Shelf reported by Moore and Krest (2004) as well as our high salinity surface water samples. The Ra enrichment in Bight bottom waters was also generally greater than can be accounted for by mixing of saline offshore waters with river waters (Figs. 3 & 4).

All Ra isotopes show lower enrichments farther away from the barrier islands (Fig. 9) suggesting input dominantly near the islands (both the MS/AL barriers as well as the Chandeleur Islands; see also grain size distribution in Supplementary Fig. S1). This should be viewed cautiously since the bottom layer was thicker farther offshore. However, the ^{224}Ra/^{228}Ra activity ratio also followed this trend (Fig. 10). Because of the short half-life of ^{224}Ra relative to ^{228}Ra, the ratio will steadily decline over a period of days to weeks. Thus, observing the ratio's highest values near the barrier islands suggests that is indeed the location of the dominant source.

We also tended to observe higher ^{228}Ra/^{226}Ra activity ratios in summer compared to spring (Fig. 10), which means that these higher ^{228}Ra/^{226}Ra activity ratios were associated with the high Ra activities (also higher Ba and Si as well as lower DO) in summer bottom water samples (Fig. 9). This is an important observation since ^{228}Ra/^{226}Ra activity ratios tended to be around 1 for both offshore waters (Reid et al., 1979) and our river samples, whereas most of our SGD samples had ratios above 2. In general, the Ra isotope distributions in Mississippi Bight bottom waters reveal distributions similar to those described in the previous section. That is, bottom water activities were higher in summer than in spring and were also especially high near the barrier islands. This similarity with other chemical distributions is also emphasized in the DO-Ra plots (Fig. 5), further suggesting a possible linkage between hypoxia and SGD. However, other factors potentially affecting Ra also require consideration.

Ra distributions do not respond directly to changes in redox conditions, since dissolved Ra only exists in the +II oxidation state. However, reducing conditions can indirectly influence the mobility of Ra through the manganese (Mn) redox cycle. Manganese oxides effectively scavenge Ra, as evidenced by the use of MnO_2-impregnated acrylic fibers to preconcentrate radium from the water column (Moore and Reid, 1973). The apparent solubility of Ra can thus increase in oxygen-deficient waters (Herczeg et al., 1988). Indeed, Garcia-Orellana et al. (2014) observed the release of radium into bottom waters in Long Island Sound (NY), which they suggested was partly due to the reductive dissolution of solid phase Mn^{4+} to Mn^{2+} in sediments or sinking particles. Barium, like Ra, is also affected by the Mn redox cycle (Charette and Sholkovitz, 2006). Therefore, the strong sorption affinity of Ra and Ba to Mn oxides stresses the need to consider the role played by Mn oxide dissolution in the increased Ra and Ba concentrations measured in Mississippi Bight hypoxic bottom waters in summer 2016. Evaluation of this issue, however, is problematic given that increased bottom water dissolved Mn could result both from a seasonally increased flux of Mn-rich anoxic SGD as well as seasonal reductive dissolution of Mn oxides near the sediment-water interface.

We did indeed observe that dissolved Mn concentrations were much

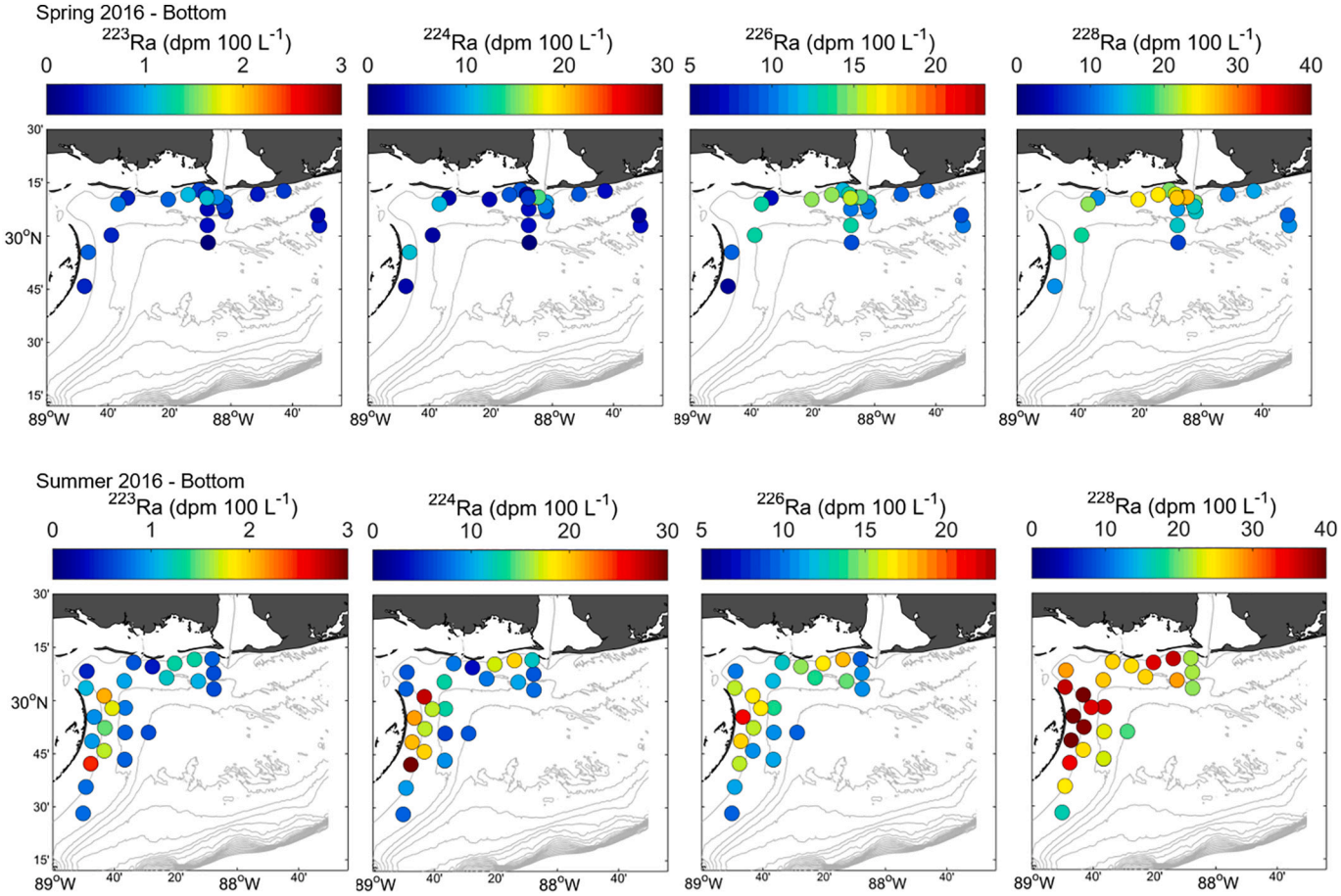

Fig. 9. Radium activities (^{223}Ra, ^{224}Ra, ^{226}Ra, ^{228}Ra) in Mississippi Bight bottom waters for spring (top) and summer (bottom) 2016. The bathymetry is shown in gray with isobaths from 10 m to 200 m; contours every 10 m.

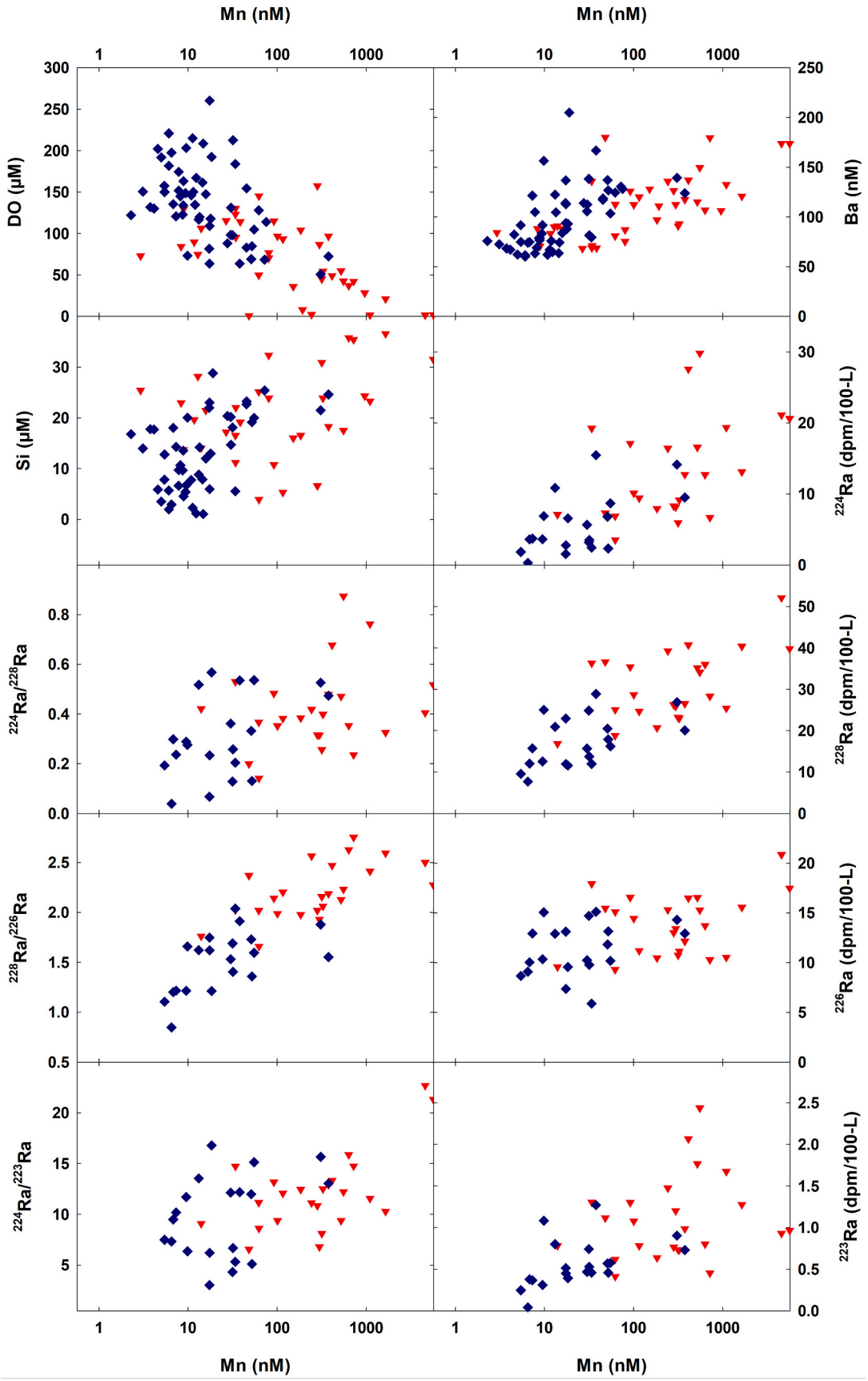

Fig. 10. Dissolved manganese concentrations (Mn) versus dissolved oxygen (DO), silicic acid (DSi), barium (Ba), Ra activities (^{223}Ra, ^{224}Ra, ^{228}Ra, ^{226}Ra), and Ra activity ratios (^{224}Ra/^{228}Ra, ^{228}Ra/^{226}Ra, ^{224}Ra/^{223}Ra) in Mississippi Bight bottom waters in spring (blue diamonds) and summer (red inverted triangles) 2016. (For interpretation of the references to colour in this figure legend, the reader is referred to the web version of this article.)

higher in the Mississippi Bight bottom waters in summer than in spring 2016 (Fig. 10), consistent with results of a multi-year time series in the northwest corner of the Bight (Ho et al., 2019). In spring, bottom water dissolved Mn ranged from 2 to 376 nM with a median value of 13 nM. The highest dissolved Mn concentrations in spring were found near Main Pass of Mobile Bay, which is also where the lowest DO concentrations were found (Supplementary Fig. S6). Relatively high dissolved Mn concentrations were also observed in the two samples collected east of the Chandeleur Islands and in general along the AL/MS barrier islands as well. In summer, the bottom dissolved Mn concentrations ranged from 3 to 5600 nM, with a median value of 96 nM, and with the highest concentrations east of the Chandeleur Islands. Dissolved Mn concentrations were usually higher in hypoxic waters than in oxic waters, consistent with the reductive dissolution of Mn oxides (Fig. 10). Additionally, bottom waters with high dissolved Mn concentrations tended to have high Ra and Ba concentrations (Fig. 10). While this is certainly compatible with the idea of release of sorbed Ra and Ba during reductive dissolution of Mn oxides, our observations suggest caution with this interpretation. First, the Mn-enriched bottom water samples are also often enriched in dissolved Si, which would not be expected to strongly sorb to Mn oxides (though it will adsorb to Fe oxides; e.g., Taylor, 1995). Even if some Si is released through reductive oxide dissolution, it seems unlikely that dissolved Mn increases of generally <2 μM could account for dissolved Si increases >20 μM (Fig. 10). Likewise, with increases of ~100 nM dissolved Mn, we see similar ~100 nM increases in dissolved Ba, an unlikely 1:1 M ratio for adsorbed Ba on Mn oxide. In Long Island Sound, Garcia-Orellana et al. (2014) observed increases of ~1 dpm 100-L^{-1} in ^{224}Ra associated with a dissolved Mn increase of ~1.8 μM: far lower than the increases in ^{224}Ra that we observe with similar or higher dissolved Mn increases. It thus seems unlikely that release of Ra and other tracers during reductive oxide dissolution in surface sediments is the dominant factor in the Ra or other SGD tracer bottom water enrichments we observe; instead, the high Mn concentrations probably reflect dissolution in deeper permeable sediments with transport to the bottom water via SGD.

On the nearby Louisiana Shelf, it has been suggested that Ra distributions might be affected by release of produced water from oil and gas extraction operations (McCoy et al., 2007). While there are more oil and gas platforms over the Louisiana Shelf, nonetheless, the Mississippi Bight, especially the southwestern corner, hosts a large number of drilling platforms and pipelines (Edelstein, 2017). For the Louisiana Shelf, Veil et al. (2005) estimated a produced water discharge of 8.1 × 10^4 m^3/d over a 1.7 × 10^4 km^2 area. If we assume a 10-day residence time of Bight bottom waters and a 5-m thick bottom layer (see modeling section), then produced waters get diluted by a factor of ~10^5. This is likely an underestimate of produced water dilution in the Bight both because of the lower density of oil/gas infrastructure in the Mississippi Bight than the Louisiana Shelf as well as the likelihood that a fraction of produced waters is discharged at or near the surface rather than the bottom. In any event, the 10^5-dilution factor means that to increase bottom water Ra by 1 dpm 100-L^{-1}, a produced water Ra activity of 10^5 dpm/100-L would be required. Note that for all of the Ra isotopes except ^{223}Ra, 1 dpm 100-L^{-1} is a minor fraction of the bottom water enrichments we observe. Reports by Kraemer and Reid (1984) and Meinhold et al. (1996) indicate maximum produced water ^{226,228}Ra activities in the Gulf of Mexico of 1–3 × 10^5 dpm 100-L^{-1}, with most discharges having much lower activities. Furthermore, the ^{228}Ra/^{226}Ra activity ratios of produced water in the northern Gulf (Kraemer and Reid, 1984) tend to be lower than most of our summer bottom water activity ratios. Thus, it seems unlikely that the Ra enrichments we observe can be significantly accounted for by produced water discharges.

The weight of the evidence is thus that the bottom water enrichments in Ra are dominantly due to input from the sediments, with fluvial sources, reductive dissolution of Mn oxides, and produced water inputs being generally minor factors. This does not tell us the specific mechanism(s) of the Ra input, which could be molecular diffusion, pore water exchange (including bio-irrigation), seawater circulation through sediments, and fresh terrestrial groundwater flow. All of these mechanisms can be encompassed by the broadest definition of SGD. However, generally in coastal/estuarine waters, molecular diffusion is thought to be of minor importance compared with other SGD mechanisms (e.g., Beck et al., 2007; Garcia-Solsona et al., 2008; Rodellas et al., 2017).

3.4. Water age estimates

After input from a source, radium isotope distributions change with time due to decay of short-lived isotopes. Two age models using different source functions have been applied: a point or line source, where the surface water becomes isolated from the source, and a continuous source, where the same input continues to occur (Moore, 2000; Moore et al., 2006). Our study area likely presents a hybrid input, with a strong source near the islands that continues but diminishes offshore. Using the point source model yields apparent ages about half those of the continuous model. Choosing a mean ^{224}Ra/^{228}Ra activity ratio of our high salinity (S > 26) barrier island SGD samples, yields a mean age for our bottom Ra samples of 7 days using the point source and 16.5 days using the continuous source model.

We can compare these estimates with dye experiments conducted during 20 days (C. Bouchard, pers. comm.) using a regional Coupled Ocean-Atmosphere-Wave-Sediment Transport (COAWST) model of the Mississippi Bight (Greer et al., 2018; Warner et al., 2010). COAWST was implemented with the CONCORDE Meteorological Analysis (CMA, Fitzpatrick and Lau, 2019). The dye experiments were based on the evolution of a conservative tracer of a concentration equal to unity (Zhang et al., 2012). The amount of conservative tracer decreased with time as the tracer-rich water was replaced by tracer-free water entering the study area, until the concentration of the conservative tracer reached 0.37 or 1/e (Jouon et al., 2006). The model estimated a residence time between 2 and 6 days (Supplementary Fig. S8) (Bouchard et al., 2020a, 2020b). Note that the residence time estimated by the model refers to the average flushing time for the whole water column, not only for the bottom waters. Nonetheless, we conclude that both Ra-based and tracer-calibrated numerical models suggest short residence times of the water. The uncertainty in these numbers leads us to adopt 10 days as a rough conservative estimate for bottom water residence time in the Bight with the realization that the residence time is undoubtedly seasonally and episodically variable (as evidenced by rapid variability in bottom water DO; Dzwonkowski et al., 2018).

3.5. Estimation of SGD rate

Quantitatively evaluating SGD is challenging because of its non-point source nature as well as its variability in space and time (Burnett et al., 2001). Estimating SGD fluxes using geochemical tracers can allow us to capture its elusive nature. The usual approach is to make a mass balance on the groundwater tracer (typically Ra isotopes) using known or assumed values of tracer concentrations in endmembers, and solve for the remaining unknown flux, which is assumed to be SGD (e.g., Beck et al., 2007; Garcia-Orellana et al., 2014; Garcia-Solsona et al., 2008). This method requires identifying a control volume and constraining as accurately as possible the sources and sinks of the tracers for this control volume.

For the Mississippi Bight, accurate mass balance modeling is problematic for a number of reasons. First, the Bight is a vertically stratified system (Supplementary Fig. S3). One might be tempted to use a control volume that includes both surface and bottom layers since both may be affected by SGD. However, the surface waters, in particular, may have acquired an SGD signal outside of the study area, for instance, in Mobile Bay (Montiel et al., 2018) or Mississippi Sound (Ho et al., 2019). Thus, including the surface waters in our control volume would likely lead to an overestimate of SGD input into the Bight bottom. A second issue with our study area is the rapid changes in the water column, largely caused

by changing wind patterns. For example, Dzwonkowski et al. (2018) show bottom DO records at several moorings in the Bight for summer 2016 stretching from several weeks before to a month after our summer survey. Bottom DO can rapidly increase or decrease, in some cases changing by >50 μM in less than a day. Such changes likely indicate rapid advection of waters in and out of the control volume thus making the residence time of water in that volume highly variable.

The unbounded nature of both the entire Bight as well as the areas near the barrier islands where our distributions suggest the most substantial SGD fluxes occur, also make it difficult to define a pertinent control volume. We could choose an outer bound near the shelf break, thereby providing a mean flux for the entire Bight. However, the limitations of the spatial distribution of samples (i.e., sparse coverage of the further offshore regions of the Bight) suggest we are better off to focus on regions near the barrier islands where both hypoxia and SGD indicators are more prevalent. This also allows us to focus on the issue of hypoxia-SGD linkage. Our unbounded study region is also problematic because in any attempt to do a mass balance, we cannot simply take river fluxes as one of our inputs, since it is not immediately clear what fraction of river discharge enters the control volume or how its composition may change as it passes through the Mississippi Sound. Furthermore, while most of the fluvial input is from Mobile Bay and other local rivers, the Mississippi River plays a seasonally and spatially changing role in contributing materials to the Bight (Sanial et al., 2019).

With these various caveats in mind, we start with a basic mass balance approach and try to discern how the complicating factors might affect our results. We start with.

$$J_{out} + J_{\lambda} = J_{est} + J_{res} + J_{diff} + J_{sw} + J_{biol} + J_{SGD} \quad (1)$$

where the J's are chemical fluxes (amount/time), the left side of the equation being removal terms and the right side being inputs. This equation assumes steady state conditions. In the equation, J_{out} is the flux of material out of the control volume, J_{λ} accounts for decay of radioactive constituents, J_{est} is fluvial input as modified by estuarine processes, J_{res} is the flux due to sediment resuspension, J_{diff} is molecular diffusion from the sediments, J_{sw} is input of material from offshore seawater, J_{biol} accounts for biological factors in bottom waters including biological uptake ($J_{biol} < 0$) as well as the remineralization of materials in the bottom water or at the sediment-water interface ($J_{biol} > 0$), and J_{SGD} is the SGD flux. As mentioned earlier, J_{SGD} might further be divided into deeply-sourced SGD with a length scale of meters to kilometers versus pore water exchange ("PEX") with a length scale shorter than meters (e.g., Cai et al., 2014; Rodellas et al., 2017; Santos et al., 2012). However, our dataset does not allow us to adequately tease apart the pore water exchange from the SGD flux.

Because of the complexities of our study area, we use two different applications of Eq. (1). The first approach applies the mass balance on one chemical distribution at a time (plus salinity and continuity) to see what insights that can provide about different element sources. The second approach uses two chemical distributions (plus salinity and continuity) to obtain more information on fluxes than the first approach can provide. Each approach also requires slightly different assumptions and thus comparing the results may allow for a test of those assumptions.

In the previous section, we noted that J_{diff}, at least for Ra, is generally minor and will be ignored. It is also possible that sediment resuspension (i.e., J_{res}) accounts for injection into bottom waters of porewaters that are enriched in Ra, Ba, and nutrients, but depleted in DO (Niemistö and Lund-Hansen, 2019; Rodellas et al., 2015b). While transmissometer profiles did occasionally show reduced light transmission near the bottom, this did not correlate with the observed constituent enrichments (and DO depletion). Indeed, during summer, lower near bottom light transmission actually correlated significantly (though with considerable scatter) with lower Ba, ^{224}Ra, and DON; i.e., opposite of what might be expected due to a resuspension effect. While these relationships may be fortuitous or result from an interplay of unresolved factors, the important point is that we cannot explain the observed bottom chemical effects through resuspension and thus J_{res} will be ignored. Temporarily, we will also ignore J_{biol}, but subsequently examine its possible importance in a later section.

3.5.1. Model 1

In the case of the Mississippi Bight bottom waters, not all of the flux of material out of surrounding fluvial/estuarine environments enters our control volume. Thus, as detailed below, we use a simple linear combination of offshore constituent concentrations and "effective" river concentrations (with the linear proportions based on salinity) to estimate the conservative inputs of these two sources to the control volume. This input is then subtracted from the observed bottom water constituent concentrations to estimate excess concentrations of materials in Bight bottom waters (i.e., the concentration we think is due to SGD).

For the input of a constituent "C" into Bight bottom waters from inflow of offshore seawater, we multiply the constituent concentration of offshore seawater (C_{SW}) by the salt fraction of bottom waters (S_B/S_{SW}) and the total flux of water out of the bottom (Q_{out}); i.e., $J_{sw} = [C_{SW}](S_B/S_{SW})Q_{out}$, where S_B and S_{SW} are the salinities of Bight bottom water and offshore seawater, respectively. Note that some SGD mass balances omit the salt fraction factor. This may be only a minor error where waters in the control volume are near the salinity of offshore seawater and/or the offshore constituent concentrations are low compared to other concentrations.

For the inflow of "C" to the Bight bottom from rivers and estuaries, one often uses measurements of river water concentrations plus an additional factor for estuarine desorption from the fluvial suspended load. Again, this is problematic for our study region because of the various fluvial sources and the fact that only some unquantified fraction of this water mixes into the Bight bottom waters. Furthermore, water passing through local estuarine environments (e.g., Mobile Bay, Mississippi Sound) may receive benthic inputs or experience biological removal before the water enters the Mississippi Bight. We therefore use our Bight surface water data to extrapolate concentration-salinity data to zero salinity and estimate an "effective" river concentration (C*; see red lines on Figs. 3, 4 and Supplementary Table S2). This is an application of the so-called "standard model" of estuarine mixing (e.g., Boyle et al., 1974; Kaul and Froelich, 1984) and is subject to a number of assumptions which are often violated (e.g., Shiller, 1996). However, many of the assumption violations (e.g., recycling traps, benthic inputs) tend to lead to an overestimate of C*, and thus would lead us to underestimate the possible effect of SGD. Furthermore, examination of our property-salinity plots (Figs. 3, 4) shows that because the Bight bottom waters tend to be very saline, large changes in our estimates of C* have a minor impact on our result. Thus, the combined freshwater and estuarine contribution to Bight bottom waters is estimated by multiplying an effective river concentration (C*) by the freshwater fraction of Bight bottom waters ($[S_{SW}\text{-}S_B]/S_{SW}$) and the total flux of water out of the bottom (Q_{out}): $J_{est} = [C^*][(S_{SW}\text{-}S_B)/S_{SW}]Q_{out}$. This formula also assumes that any fresh groundwater being discharged into the Bight bottom waters is a minor component of the overall water budget, which is generally the case (e.g., Burnett et al., 2006). Because groundwater concentrations are typically at least an order of magnitude greater than bottom water concentrations, we neglect the transport of bottom water into the sediments in the budget.

Using $J_{out} = C_B Q_{out}$, where C_B is the constituent concentration in Bight bottom waters and, for radioactive constituents, $J_{\lambda} = C_B \lambda V$, where λ is the pertinent radiodecay constant and V is the volume of the system, we rewrite Eq. (1) as:

$$Q_{out}\{C_B - [C_{SW}](S_B/S_{SW}) - [C^*][(S_{SW} - S_B)/S_{SW}]\} + C_B \lambda V = J_{res} + J_{diff} + J_{biol} + J_{SGD} \quad (2)$$

where the terms on the left of the equals sign are our representation of

J_{out} - J_{sw} - J_{est} + J_{λ}. The quantity in curly brackets can be termed the excess concentration of C in Bight bottom waters. We make two more modifications to this equation. First, following many other SGD box models, we substitute V/T for Q_{out}, where T is the residence time of water in the control volume. We also use h, the mean thickness of the Bight bottom layer as determined from our CTD profiles, rather than the volume (V), which changes the units of the various terms from amount/time to amount/time/area.

We apply Eq. (2) to three different regions of the Bight for both our spring and summer data. The three regions include 1) a box south of the Mississippi-Alabama barrier islands, extending west from 88.1°W (approx. Main Pass, Mobile Bay) and north of 30.09°N (Fig. 1), 2) a box east of the Chandeleur Islands, extending south of 30.09°N and west of 88.6°W (Fig. 1), and 3) all other samples (i.e., locations away from the barrier islands). Several spring samples near the Chandeleurs were eliminated because CTD profiles did not show a clear separation between shallow and deep layers or because chemical sampling missed the bottom layer. Also, for both spring and summer, several bottom water samples were excluded from our analysis due to evidence from CTD profiles that there had been recent significant vertical mixing and there was no relatively homogeneous bottom layer.

The model was applied to our data for the radium quartet along with Ba and nutrients. We made both high and low estimates of C* since there was considerable variability in surface water concentrations (see red lines in Figs. 3 & 4). The thickness of the bottom enriched layer (h) was estimated for each region of interest and for both seasons from CTD profiles, and varied between 3 and 7 m. We chose a nominal 10-day residence time (T) of water in the bottom layer as described in the previous section and further examined below.

As noted above (Section 3.2), because bottom waters did not show a significant freshwater signature, we used the chemical composition of the saline groundwater samples to estimate the SGD endmember concentrations for the model.

Estimates of SGD rates from these calculations are shown in Fig. 11 with further detail in Supplementary Table S3. With the caveats above in mind, we can draw some preliminary conclusions. Radium-based estimates of SGD flux are fairly convergent with an average of 0.045 ± 0.005 $m^3\ m^{-2}\ d^{-1}$ (Standard Error), which includes both seasons and the three regions of interest. If we assume that ^{224}Ra and ^{228}Ra provide the best estimates of SGD flux, this results in mean spring and summer flux rates of 0.036 and 0.059 $m^3\ m^{-2}\ d^{-1}$, respectively. These values are similar in magnitude to estimates of SGD flux in other coastal waters of the northern Gulf of Mexico (Cable et al., 1996; Kolker et al., 2013; McCoy and Corbett, 2009). There is more variability in the results of the ^{226}Ra-based estimates than for the other Ra isotopes: this is not surprising since the data (Fig. 4) show that ^{226}Ra is less enriched in Bight bottom waters relative to C* and offshore waters than the other isotopes. Therefore, we do not include estimates based on ^{226}Ra. We also note that the ^{223,224,228}Ra and Ba-estimated SGD flux near the Chandeleur Islands in summer was greater than other SGD flux estimates, spatially and temporally. It was also near the Chandeleurs in summer that we observed the greatest hypoxia. Finally, SGD flux estimates based on summer nutrient distributions (Supplementary Table S3) were generally higher than the Ra-based estimates. This is likely due to our not accounting for regeneration of these elements in bottom waters or at the sediment-water interface, an issue we return to in a subsequent section.

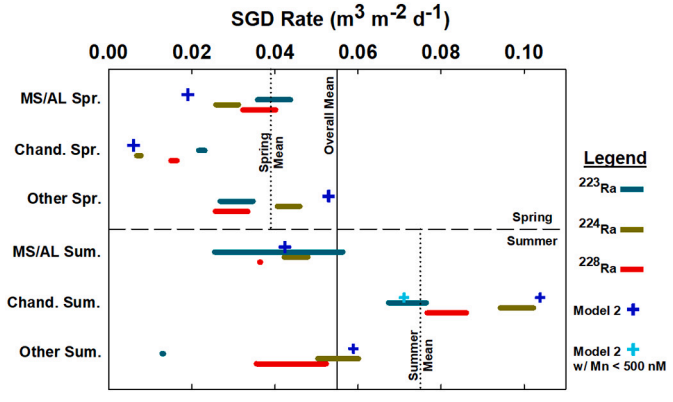

Fig. 11. Submarine groundwater discharge (SGD) rate for spring and summer 2016 for the three regions of interest in the Mississippi Bight: south of the MS/AL barrier islands (MS/AL), east of the Chandeleur Islands (Chand), and the remaining outlying samples gathered in a third group "Other". The estimates of SGD rate are from the two models. The black line and shaded region represent the average SGD rate and the standard deviation (excluding the Si value) for this study.

As an alternative approach to the calculation, we tuned the model by adjusting the water residence time to force the ^{224}Ra and ^{228}Ra SGD water flux estimates to agree. For spring, this resulted in a residence time of 10 days and a ^{224,228}Ra SGD flux of 0.035 $m^3\ m^{-2}\ d^{-1}$, suggesting that the 10-day residence time estimate is reasonable. For summer, the result of the tuning approach is a residence time of 6.2 days and a ^{224,228}Ra SGD flux of 0.092 $m^3\ m^{-2}\ d^{-1}$. This residence time is lower than the 10 days assumed above, but similar to COAWST model predictions described earlier.

3.5.2. Model 2

Our second model again focuses on the mass balance in Bight bottom waters. This model simultaneously solves four mass balances applied to the Bight bottom waters in order to obtain values for the water fluxes in and out of the control volume. The equations include a mass balance on a short-lived Ra isotope (i.e., ^{224}Ra) which includes a decay term (Eq. (3)), a mass balance on a long-lived Ra isotope (i.e., ^{228}Ra) which therefore needs no decay term in coastal waters (Eq. (4)), a mass balance on salinity (Eq. (5)), and a continuity equation (Eq. (6)). As with the previous model, we start off by assuming that $J_{res} + J_{diff} + J_{biol}$ terms can be ignored. The pertinent equations are:

$$Q_{out}{}^{224}Ra_B + \lambda V{}^{224}Ra_B = Q_{sw}{}^{224}Ra_{sw} + Q_{sfc}{}^{224}Ra_{sfc} + Q_{SGD}{}^{224}Ra_{SGD} \quad (3)$$

$$Q_{out}{}^{228}Ra_B = Q_{sw}{}^{228}Ra_{sw} + Q_{sfc}{}^{228}Ra_{sfc} + Q_{SGD}{}^{228}Ra_{SGD} \quad (4)$$

$$Q_{out}S_B = Q_{sw}S_{sw} + Q_{sfc}S_{sfc} + Q_{SGD}S_{SGD} \quad (5)$$

$$Q_{out} = Q_{sw} + Q_{sfc} + Q_{SGD} \quad (6)$$

where the Q's are water fluxes out of the bottom water (Q_{out}), and into the bottom from offshore (Q_{sw}), the surface (Q_{sfc}), or from SGD (Q_{SGD}). Given values for the Ra isotopes and salinity in the bottom waters and the three sources, this system of equations can readily be solved by matrix inversion. As before, we consider spring and summer separately as well as the three regions of the Bight described in the previous section. Additional limitations of this model include the scatter in the data as well as spatial/temporal uncertainties in the groundwater endmember concentrations.

Results for this model indicate a similar magnitude of SGD water flux (0.060 ± 0.014 $m^3\ m^{-2}\ d^{-1}$ [S.E.]) as the first model, with spring rates (0.045 $m^3\ m^{-2}\ d^{-1}$) being lower than summer (0.075 $m^3\ m^{-2}\ d^{-1}$) and the highest rate again being near the Chandeleur Islands in summer. In general, these calculations are more sensitive to uncertainties in ^{224}Ra concentrations than in ^{228}Ra or S. Use of ^{223}Ra in place of ^{224}Ra yields similar results, though the lower ^{223}Ra concentrations result in greater uncertainty. Likewise, use of ^{226}Ra in place of ^{228}Ra in the calculation yields even greater uncertainty in the results and is particularly sensitive to the choice of ^{226}Ra endmember concentrations. Another output of the model is the residence time. Using the ^{224}Ra results indicates a mean residence time of 7.8 days in spring and 10.3 days in summer. Again, these results are in general accord with our use of a 10-day overall average.

Besides the flux of SGD, this model allows estimation of other water fluxes and hence the ratios of Q_{SGD}/Q_{out} and Q_{sfc}/Q_{out}. Our model suggests that Q_{SGD} is as much as 10–20% (mean 12%) of the total inflowing water budget of the Bight bottom, again emphasizing that it is the material in the SGD, rather than the water itself, that is important. Of course, since SGD is generally dominated by circulated seawater, there is likely little or no net gain of water. Additionally, typically Q_{sfc} is only about 14% of the total inflowing water budget of the Bight bottom. Thus, the flux of offshore salty water through these coastal bottom waters is roughly three-fourths of the water balance. As noted elsewhere, this flux of salty offshore bottom water is an important and generally unquantified vector of coastal material transport (Shiller, 1996). Our model thus also provides a possible alternative to excess ^{210}Pb inventories (Smoak et al., 1996) as a means of estimating this flux of salty offshore bottom water.

As noted in the Ra distribution discussion (Section 3.3), our data indicate that dissolved Mn was often high in hypoxic summer bottom waters, sometimes over 1 μM. While we argued above that release of adsorbed Ra during reductive dissolution of Mn oxides was not likely a dominant factor controlling the Bight bottom water Ra, we can now use our model to further test this. Specifically, we eliminated all samples from the Chandeleur control volume that had dissolved Mn >500 nM and recalculated the SGD estimate (The average dissolved Mn of the remaining samples was 168 nM). While the estimated SGD flux did decrease by ~30% (Fig. 11), nonetheless it was still elevated relative to SGD flux estimates for spring and for the rest of the Bight during summer. Here again, the conclusion is that the Mn oxide effect on the Ra distribution is not a dominant factor.

We again emphasize that the SGD flux estimated from our two models (0.055 ± 0.009 m^3 m^{-2} d^{-1}) is within the range of previous estimates from SGD studies conducted along the coast of the northern Gulf of Mexico (McCoy and Corbett, 2009; and therein). Montiel et al. (2018) likewise estimated a total groundwater flux (fresh and saline) in Mobile Bay, Alabama, between 0.004 and 0.028 m^3 m^{-2} d^{-1} depending on the season and the location in Mobile Bay.

3.6. Contribution to Bight Nutrient fluxes

The potentially wide spatial range over which SGD occurs in the northern Gulf could generate large nutrient inputs and also have consequences on the oxygen demand. Two related methods can be used to estimate SGD nutrient fluxes to Bight bottom waters. One can multiply the SGD nutrient/^{228}Ra ratios by the SGD flux of ^{228}Ra. That ^{228}Ra SGD flux is calculated using the excess ^{228}Ra in the bottom water along with a bottom water residence time and thickness of the bottom layer (i.e., Model 1). Alternatively, one can multiply the average SGD water flux by the SGD nutrient concentrations. Similar results are obtained since the methods fundamentally use the same data. Mean fluxes (averaged over the Bight for both seasons) are shown in Table 1. Interestingly, our fluxes are similar in magnitude to DIP, DSi, and NH_4^+ fluxes determined during benthic lander deployments in the Bight during August 2011 (Berelson et al., 2019). This nutrient input delivered into Bight bottom waters potentially could stimulate benthic primary production. In fact, high Chl-a concentrations were found in spring bottom water for samples displaying unusually low DIN/^{228}Ra ratios (Supplementary Fig. S9). Interestingly, SGD nutrient input tends to have a lower DIN:DIP ratio than river waters, thus suggesting other possible differences in the ecosystem effects of these two nutrient sources.

Comparing the SGD nutrient fluxes with river nutrient fluxes is somewhat challenging since the river flux enters the surface waters and then disperses over a broad area. However, the salinity-nutrient trends (Figs. 3 & 4) make it clear that river input is unlikely to directly input a substantial nutrient flux to the saline bottom waters. We make a rough comparison of SGD and fluvial nutrient fluxes as follows. We assume the SGD flux primarily occurs in an 'L' shaped box extending ~17 km seaward from the MS/AL barrier islands and the Chandeleurs (Fig. 1).

Table 1
Submarine Groundwater Discharge (SGD) rates of different constituents to the Mississippi Bight.

	SGD Flux[1]	SGD Flux[2]	Local River Flux[3]	Benthic Lander Flux[4]
	(mmol/m^2/d)	(kmol/d)	(kmol/d)	(mmol/m^2/d)
Ba	0.018	0.42	48	
DIN	2.0	47	3300	
DON	2.2	51	6500	
NH_4^+	1.5	34		2.7–5.7
TDN	4.2	98	9800	
DSi	7.9	183	8640	7.7–9.6
DIP	0.20	4.6	110	0.10–0.23
CH_4	0.017	0.39		

[1] Based on mean estimated SGD composition (Section 3.1) and 0.055 m^3/m^2/d seepage rate; estimates based on mean ^{228}Ra flux (68 dpm/m^2/d) and constituent/^{228}Ra SGD ratios are ~12% lower.
[2] Based on L-shaped box extending 10–15 km from barrier islands = 2×10^9 m^2.
[3] Based on mean local river composition (Section 3.1) and mean discharge of 2500 m^3/s.
[4] From Berelson et al., 2019.

This gives an area of $\sim 2 \times 10^9$ m^2, which ignores much of the Bight and thus underestimates the area of SGD input and hence the contribution of SGD nutrients to our comparison. For the rivers, isotopic data suggests that fresh water in the Bight was dominantly from local rivers rather than the Mississippi River during our spring/summer surveys (Sanial et al., 2019). We thus use an average annual local river discharge of 2500 m^3/s (Dzwonkowski et al., 2018) and our measured river nutrient concentrations (Section 3.1) to estimate a river flux of nutrients. This likely overestimates the fluvial nutrient input to the Bight since it assumes all of the fluvial nutrients enter the Bight and ignores both wider coastal dispersion of the river flow as well as nutrient removal in local bays and the Mississippi Sound. The important result (Table 1) is that these two nutrient fluxes (SGD and fluvial) have similar magnitudes. Since our simple calculation probably minimizes SGD input and maximizes fluvial input, one is left with the conclusion that SGD nutrient input is a substantial contributor to the biogeochemistry of the Mississippi Bight.

Despite this conclusion of the significance of SGD nutrient inputs, we have to this point largely ignored another important way that fluvial (or other allochthonous) nutrients could contribute to bottom water nutrient excesses: through surface water biological uptake of fluvial nutrients and subsequent sinking and regeneration in the bottom waters, i.e., the J_{biol} term in Eq. (1). If we assume that biological cycling is a minimal factor for Ra, then we can compare the SGD nutrient fluxes estimated above, with fluxes calculated simply from the bottom water nutrient excesses, the residence time, and the bottom layer thickness. The ratio of the two flux estimates reduces to:

$$\mathrm{SGD\%} = 100\% \times \left([\mathrm{Nutrient}]/[^{228}\mathrm{Ra}]\right)_{\mathrm{SGD}} \Big/ \left([\mathrm{Nutrient}]/[^{228}\mathrm{Ra}]\right)_{\mathrm{BW-excess}}$$

In other words, this is simply a comparison between concentration ratios and does not depend on estimates of the thickness or residence time of the bottom layer. A ratio of 100% implies that SGD dominates nutrient input to the bottom waters and that regeneration of nutrients derived from the surface has minimal impact on the bottom nutrient mass balance, while a ratio of 50% implies that half of the bottom nutrient excess is from SGD and half from regeneration. Variability in SGD composition as well as the extent of SGD input versus regeneration input makes it difficult to do a precise comparison. For example, the $([Si]/[^{228}Ra])_{SGD}$ ratio in our high salinity (S > 26) groundwater samples varied from 13 to 550 μmol/dpm, while the $([Si]/[^{228}Ra])_{BW\text{-}excess}$ ratio in summer bottom water varied from 9 to 1050 μmol/dpm. That said, a comparison of the SGD% values for the nutrients is instructive, so long as one remembers the significant uncertainty in the absolute numbers. During the spring, the average SGD% values were 92, 113, and

79% for DIP, DSi, and TDN, respectively. During summer, the average SGD% values were 11, 43, and 35% for DIP, DSi, and TDN, respectively. These numbers suggest the possibility that SGD is the dominant contributor to bottom nutrients during spring but that the relative importance of regeneration increases during summer. This is compatible with the idea of a couple month lag between spring surface water primary productivity and subsequent bottom regeneration (e.g., Justić et al., 1993). Nonetheless, summer SGD nutrient inputs remain a substantial ecosystem factor, especially given that our models suggest higher SGD flux rates during summer than spring.

3.7. Oxygen demand

Peterson et al. (2016) observed low DO bottom waters (<60% saturation) near Myrtle Beach, SC, were associated with Ra contents indicative of substantial SGD influence (30–60%). Our model 2 suggests the fraction of SGD influence in Bight bottom waters was 10–20% during spring/summer 2016. In order for a 10–20% fraction of zero oxygen SGD to result in bottom hypoxia (DO = 62.5 μM), the bottom water would have to have started with a DO of only 69–78 μM prior to the input of the SGD. Thus, input of zero oxygen SGD to Bight bottom waters might push a primed system into hypoxia but would probably not be the dominant driving force for establishment of hypoxia. However, SGD is essentially a negative DO input, since the reduced species within it (e.g., NH_4^+) represent an oxygen demand.

In our samples, we determined NH_4^+ and DON, both of which require two O_2 molecules for oxidation to nitrate. Methane likewise has a 2:1 stoichiometric oxidation ratio, though its concentrations appear to be too low in our SGD to have a significant DO demand. The organic carbon associated with the DON will also have an oxygen demand (1:1) and we conservatively use a C:N ratio of 117:16 (Anderson and Sarmiento, 1994) to convert our DON fluxes to DOC. Note, however, that benthic DOM is often considerably more N-poor than this (e.g., C:N ~ 200; Rasheed et al., 2004) and, thus, we likely significantly underestimate the DOC flux. Using the results of our model 2 calculations and our saline SGD endmember composition, we can thus estimate potential DO demand from SGD during the residence time of bottom waters. We call this the *potential DO demand* since we are uncertain the extent to which oxidation of these reduced SGD constituents occurs in bottom waters. During spring 2016, we find a potential DO demand of 39 μM in the region near the barrier islands and 22 μM further offshore. In summer 2016, the potential DO demand increased to 78 μM near the barrier islands and 33 μM offshore.

Our analysis clearly shows that that the DO demand of reducing SGD constituents could have a significant impact on the development of hypoxia in Mississippi Bight bottom waters. The potential DO demand is higher near the barrier islands than offshore, and higher in summer than in spring. These observations are in agreement with both when and where we see the most significant bottom water DO depletion.

4. Conclusion

SGD has increasingly been understood to play an important role in the biogeochemistry of coastal ecosystems (e.g., Burnett et al., 2003; Charette and Sholkovitz, 2006; Moore and Shaw, 2008). Unlike point sources of chemical constituents, however, SGD can be spatially diffuse, with multiple sources and poorly understood temporal variability. In the Mississippi Bight, prior observations (e.g., Ho et al., 2019; Kolker et al., 2013; Krest et al., 1999; Liefer et al., 2014) led us to hypothesize that SGD might be an overlooked aspect of the biogeochemistry of that system. However, understanding the contribution of SGD in the Mississippi Bight is particularly complex due to the system's stratified nature, its occasionally rapid temporal changes, the input of waters already influenced by SGD input in nearshore bays and sounds, and the possible influence from the Mississippi River versus more local rivers having different nutrient contents. Nonetheless, distributions of Ra isotopes, Ba, nutrients, and methane in Bight bottom waters demand a significant SGD contribution. Two different approaches to modeling the bottom water Ra distribution both suggest a seepage rate of ~0.055 $m^3\ m^{-2}\ d^{-1}$, in line with previous estimates in similar systems. Our more complex model, involving four mass balances, suggests that as much as 10–20% of the bottom water in the Bight circulates through the underlying permeable sediments on the time scale of ~10 days. This circulated water emerges as SGD with a completely different chemical composition. Our model also provides a means of estimating the transport of salty offshore water through the shelf bottom waters (Shiller, 1996; Smoak et al., 1996).

Although details of the overall spatial and temporal variability of SGD composition in the Bight remain elusive, SGD appears to be a major factor in the nutrient biogeochemistry of this system. Specifically, SGD appears to be the dominant contributor of nutrients to Bight bottom waters at certain times of the year. Correlated increases in SGD indicators with declining bottom DO concentrations likewise suggest the influence of SGD on hypoxia in this system. Estimates of the potential oxygen demand of reduced species within SGD are shown to contribute significantly to the development of seasonal hypoxia in Bight bottom waters. Additional work is needed to better resolve sources of nutrients and reduced species within the Mississippi Bight SGD as well as the variability and pathways of this supply.

The bottom-up input of SGD in the Mississippi Bight thus appears to be a significant and overlooked aspect of this system. We suggest that such a bottom-up influence may be a generally important feature of coastal ecosystems. Indeed, preliminary work suggests that SGD influences bottom water hypoxia in the Changjiang (Yangtze) River estuary, perhaps by a mechanism similar to that suggested here (Guo et al., 2020). Thus, even shelves impacted by major river systems may not be immune to bottom-up SGD influences.

Declaration of Competing Interest

None.

Acknowledgements

We thank the captain and crew of the R/V Point Sur. We also thank the science party from the CONCORDE program for their help collecting the samples and their discussion. A special thanks to Melissa Gilbert and Hannah Box for analyzing most of the samples and to Peng Ho, Allison Mojzis, Laura Whitmore, and Kevin Martin for aid in collecting the CONCORDE samples. Nutrient analyses were provided courtesy of Jeff Krause, DISL; and COAWST residence times were calculated by Courtney Bouchard. This research was made possible by a grant from the Gulf of Mexico Research Initiative.

All data are publicly available through the Gulf of Mexico Research Initiative Information & Data Cooperative (GRIIDC) at https://data.gulfresearchinitiative.org (Fall 2015 doi:https://doi.org/10.7266/N7F769NC, BCS 2016 doi:https://doi.org/10.7266/N75T3J3B, Spring 2016 doi:https://doi.org/10.7266/n7-9wex-sg48, Summer 2016 doi:https://doi.org/10.7266/n7-f91t-7725, Rivers: doi:https://doi.org/10.7266/n7-sps7-rq23; Groundwater: doi: https://doi.org/10.7266/VB1D64CQ).

Appendix A. Supplementary data

Supplementary data to this article can be found online at https://doi.org/10.1016/j.marchem.2021.104007.

References

Allison, M.A., Demas, C.R., Ebersole, B.A., Kleiss, B.A., Little, C.D., Meselhe, E.A., Powell, N.J., Pratt, T.C., Vosburg, B.M., 2012. A water and sediment budget for the lower Mississippi–Atchafalaya River in flood years 2008–2010: implications for

sediment discharge to the oceans and coastal restoration in Louisiana. J. Hydrol. 432–433, 84–97. https://doi.org/10.1016/j.jhydrol.2012.02.020.
Anderson, L.A., Sarmiento, J.L., 1994. Redfield ratios of remineralization determined by nutrient data analysis. Global Biogeochem. Cycles 8, 65–80. https://doi.org/10.1029/93GB03318.
Androulidakis, Y.S., Kourafalou, V.H., 2013. On the processes that influence the transport and fate of Mississippi waters under flooding outflow conditions. Ocean Dyn. 63, 143–164. https://doi.org/10.1007/s10236-012-0587-8.
Beck, A.J., Rapaglia, J.P., Cochran, J.K., Bokuniewicz, H.J., 2007. Radium mass-balance in Jamaica Bay, NY: evidence for a substantial flux of submarine groundwater. Mar. Chem. 106, 419–441. https://doi.org/10.1016/j.marchem.2007.03.008.
Berelson, W.M., McManus, J., Severmann, S., Rollins, N., 2019. Benthic fluxes from hypoxia-influenced Gulf of Mexico sediments: impact on bottom water acidification. Mar. Chem. 209, 94–106. https://doi.org/10.1016/j.marchem.2019.01.004.
Bishop, J.M., Glenn, C.R., Amato, D.W., Dulai, H., 2015. Effect of land use and groundwater flow path on submarine groundwater discharge nutrient flux. J. Hydrol. Reg. Stud. https://doi.org/10.1016/j.ejrh.2015.10.008.
Bouchard, C., Dinniman, M., Armstrong, B., Wiggert, J., 2020a. Physical Model of the Mississippi Sound and Bight, from March 15 to May 14, 2016 with Eulerian Dye Tracer Releases for Residence Time Assessment. Texas A&M University-Corpus Christi, Gulf of Mexico Research Initiative Information and Data Cooperative (GRIIDC), Harte Research Institute. https://doi.org/10.7266/FC2783SM.
Bouchard, C., Dinniman, M., Armstrong, B., Wiggert, J., 2020b. Physical Model of the Mississippi Sound and Bight, from July 14 to October 12, 2016 with Eulerian Dye Tracer Releases for Residence Time Assessment. Texas A&M University-Corpus Christi, Gulf of Mexico Research Initiative Information and Data Cooperative (GRIIDC), Harte Research Institute. https://doi.org/10.7266/VFEKKPB0.
Boyle, E., Collier, R., Dengler, A.T., Edmond, J.M., Ng, A.C., Stallard, R.F., 1974. On the chemical mass-balance in estuaries. Geochim. Cosmochim. Acta 38, 1719–1728. https://doi.org/10.1016/0016-7037(74)90188-4.
Boyle, E.A., Reid, D.F., Huested, S.S., Hering, J., 1984. Trace metals and radium in the Gulf of Mexico: an evaluation of river and continental shelf sources. Earth Planet. Sci. Lett. 69, 69–87. https://doi.org/10.1016/0012-821X(84)90075-X.
Breitburg, D., Levin, L.A., Oschlies, A., Grégoire, M., Chavez, F.P., Conley, D.J., Garçon, V., Gilbert, D., Gutiérrez, D., Isensee, K., Jacinto, G.S., Limburg, K.E., Montes, I., Naqvi, S.W.A., Pitcher, G.C., Rabalais, N.N., Roman, M.R., Rose, K.A., Seibel, B.A., Telszewski, M., Yasuhara, M., Zhang, J., 2018. Declining oxygen in the global ocean and coastal waters. Science 359, eaam7240. https://doi.org/10.1126/science.aam7240.
Brunner, C.A., Beall, J.M., Bentley, S.J., Furukawa, Y., 2006. Hypoxia hotspots in the Mississippi Bight. J. Foraminifer. Res. 36, 95–107. https://doi.org/10.2113/36.2.95.
Brzezinski, M.A., Nelson, D.M., 1995. The annual silica cycle in the Sargasso Sea near Bermuda. Deep Sea Res. Part Oceanogr. Res. Pap. 42, 1215–1237. https://doi.org/10.1016/0967-0637(95)93592-3.
Burnett, W.C., Taniguchi, M., Oberdorfer, J., 2001. Measurement and significance of the direct discharge of groundwater into the coastal zone. J. Sea Res. 46, 109–116. https://doi.org/10.1016/S1385-1101(01)00075-2 (Land-Ocean Interactions in the Coastal Zone).
Burnett, W.C., Bokuniewicz, H., Huettel, M., Moore, W.S., Taniguchi, M., 2003. Groundwater and pore water inputs to the coastal zone. Biogeochemistry 66, 3–33. https://doi.org/10.1023/B:BIOG.0000006066.21240.53.
Burnett, W.C., Aggarwal, P.K., Aureli, A., Bokuniewicz, H., Cable, J.E., Charette, M.A., Kontar, E., Krupa, S., Kulkarni, K.M., Loveless, A., Moore, W.S., Oberdorfer, J.A., Oliveira, J., Ozyurt, N., Povinec, P., Privitera, A.M.G., Rajar, R., Ramessur, R.T., Scholten, J., Stieglitz, T., Taniguchi, M., Turner, J.V., 2006. Quantifying submarine groundwater discharge in the coastal zone via multiple methods. Sci. Total Environ. 367, 498–543. https://doi.org/10.1016/j.scitotenv.2006.05.009.
Cable, J.E., Burnett, W.C., Chanton, J.P., Weatherly, G.L., 1996. Estimating groundwater discharge into the northeastern Gulf of Mexico using radon-222. Earth Planet. Sci. Lett. 144, 591–604. https://doi.org/10.1016/S0012-821X(96)00173-2.
Cai, P., Shi, X., Moore, W.S., Peng, S., Wang, G., Dai, M., 2014. 224Ra:228Th disequilibrium in coastal sediments: implications for solute transfer across the sediment-water interface. Geochim. Cosmochim. Acta 125, 68–84. https://doi.org/10.1016/j.gca.2013.09.029.
Carpenter, S.R., Kitchell, J.F., Hodgson, J.R., 1985. Cascading trophic interactions and Lake productivity. BioScience 35, 634–639. https://doi.org/10.2307/1309989.
Charette, M.A., Sholkovitz, E.R., 2006. Trace element cycling in a subterranean estuary: Part 2. Geochemistry of the pore water. Geochim. Cosmochim. Acta 70, 811–826. https://doi.org/10.1016/j.gca.2005.10.019.
Charette, M.A., Buesseler, K.O., Andrews, J.E., 2001. Utility of radium isotopes for evaluating the input and transport of groundwater-derived nitrogen to a Cape Cod estuary. Limnol. Oceanogr. 46, 465–470. https://doi.org/10.4319/lo.2001.46.2.0465.
Collier, R., Edmond, J., 1984. The trace element geochemistry of marine biogenic particulate matter. Prog. Oceanogr. 13, 113–199. https://doi.org/10.1016/0079-6611(84)90008-9.
Diaz, R.J., 2001. Overview of hypoxia around the world. J. Environ. Qual. 30, 275–281. https://doi.org/10.2134/jeq2001.302275x.
Diaz, R.J., Rosenberg, R., 1995. Marine benthic hypoxia: a review of its ecological effects and the behavioural responses of benthic macrofauna. Oceanogr. Lit. Rev. 12, 1250.
Donner, S.D., Coe, M.T., Lenters, J.D., Twine, T.E., Foley, J.A., 2002. Modeling the impact of hydrological changes on nitrate transport in the Mississippi River Basin from 1955 to 1994. Glob. Biogeochem. Cycles 16, 16. https://doi.org/10.1029/2001GB001396.
Dortch, M.S., Zakikhani, M., Noel, M.R., Kim, S.-C., 2007. Application of a Water Quality Model to Mississippi Sound to Evaluate Impacts of Freshwater Diversions (No. ERDC/EL-TR-07-20). US Army Corps of Engineers.
Duncan, T., Shaw, T.J., 2003. The mobility of rare earth elements and redox sensitive elements in the groundwater/seawater mixing zone of a shallow coastal aquifer. Aquat. Geochem. 9, 233–255. https://doi.org/10.1023/B:AQUA.0000022956.20338.26.
Dunn, D.D., 1996. Trends in Nutrient Inflows to the Gulf of Mexico from Streams Draining the Conterminous United States, 1972–93 (No. 96–4113). Water Resources Investigations Report 96-4113 USGS.
Dzwonkowski, B., Park, K., Kyung Ha, H., Graham, W.M., Hernandez, F.J., Powers, S.P., 2011. Hydrographic variability on a coastal shelf directly influenced by estuarine outflow. Cont. Shelf Res. 31, 939–950. https://doi.org/10.1016/j.csr.2011.03.001.
Dzwonkowski, B., Greer, A.T., Briseño-Avena, C., Krause, J.W., Soto, I.M., Hernandez, F. J., Deary, A.L., Wiggert, J.D., Joung, D., Fitzpatrick, P.J., O'Brien, S.J., Dykstra, S.L., Lau, Y., Cambazoglu, M.K., Lockridge, G., Howden, S.D., Shiller, A.M., Graham, W. M., 2017. Estuarine influence on biogeochemical properties of the Alabama shelf during the fall season. Cont. Shelf Res. 140, 96–109. https://doi.org/10.1016/j.csr.2017.05.001.
Dzwonkowski, B., Fournier, S., Reager, J.T., Milroy, S., Park, K., Shiller, A.M., Greer, A. T., Soto, I., Dykstra, S.L., Sanial, V., 2018. Tracking Sea surface salinity and dissolved oxygen on a river-influenced, seasonally stratified shelf, Mississippi Bight, northern Gulf of Mexico. Cont. Shelf Res. 169, 25–33. https://doi.org/10.1016/j.csr.2018.09.009.
Edelstein, K., 2017. Oil and Gas Development in the Gulf of Mexico. US Bureau of Ocean Energy Management [WWW Document]. URL. https://maps.fractracker.org/latest/?appid=0b3260e4417d4299b750b6b2447d7f33 (accessed 7.29.19).
Fitzpatrick, P., Lau, Y., 2019. CONCORDE Meteorological Analysis (CMA) Data along the Northern Gulf Coast between April 2015 and December 2016. Distributed by: Gulf of Mexico Research Initiative Information and Data Cooperative (GRIIDC), Harte Research Institute, Texas A&M University-Corpus Christi. https://doi.org/10.7266/N72F7KHX.
Garcia-Orellana, J., Cochran, J.K., Bokuniewicz, H., Daniel, J.W.R., Rodellas, V., Heilbrun, C., 2014. Evaluation of ^{224}Ra as a tracer for submarine groundwater discharge in Long Island Sound (NY). Geochim. Cosmochim. Acta 141, 314–330. https://doi.org/10.1016/j.gca.2014.05.009.
Garcia-Solsona, E., Masqué, P., Garcia-Orellana, J., Rapaglia, J., Beck, A.J., Cochran, J. K., Bokuniewicz, H.J., Zaggia, L., Collavini, F., 2008. Estimating submarine groundwater discharge around Isola La Cura, northern Venice Lagoon (Italy), by using the radium quartet. Mar. Chem. 109, 292–306. https://doi.org/10.1016/j.marchem.2008.02.007 (Measurement of Radium and Actinium Isotopes in the marine environment).
Gonneea, M.E., Mulligan, A.E., Charette, M.A., 2013. Seasonal cycles in radium and barium within a subterranean estuary: implications for groundwater derived chemical fluxes to surface waters. Geochim. Cosmochim. Acta 119, 164–177. https://doi.org/10.1016/j.gca.2013.05.034.
Greene, D.L., Rodriguez, A.B., Anderson, J.B., 2007. Seaward-branching coastal-plain and Piedmont Incised-Valley systems through Multiple Sea-level cycles: late quaternary examples from Mobile Bay and Mississippi Sound, U.S.A. J. Sediment. Res. 77, 139–158. https://doi.org/10.2110/jsr.2007.016.
Greer, A., Shiller, A., Hofmann, E., Wiggert, J., Warner, S., Parra, S., Pan, C., Book, J., Joung, D., Dykstra, S., Krause, J., Dzwonkowski, B., Soto, I., Cambazoglu, K., Deary, A., Briseño-Avena, C., Boyette, A., Kastler, J., Sanial, V., Hode, L., Nwankwo, U., Chiaverano, L., O'Brien, S., Fitzpatrick, P., Lau, Y., Dinniman, M., Martin, K., Ho, P., Mojzis, A., Howden, S., Hernandez, F., Church, I., Miles, T., Sponaugle, S., Moum, J., Arnone, R., Cowen, R., Jacobs, G., Schofield, O., Graham, W., 2018. Functioning of coastal river-dominated ecosystems and implications for oil spill response: from observations to mechanisms and models. Oceanography 31. https://doi.org/10.5670/oceanog.2018.302.
Guo, X., Xu, B., Burnett, W.C., Wei, Q., Nan, H., Zhou, S., Charette, M.A., Lian, E., Chen, G., Yu, Z., 2020. Does submarine groundwater discharge contribute to summer hypoxia in the Changjiang (Yangtze) River Estuary? Sci. Total Environ. 719, 137450. https://doi.org/10.1016/j.scitotenv.2020.137450.
Herczeg, A.L., James Simpson, H., Anderson, R.F., Trier, R.M., Mathieu, G.G., Deck, B.L., 1988. Uranium and radium mobility in groundwaters and brines within the delaware basin, Southeastern New Mexico, U.S.A. Chem. Geol. Isot. Geosci. Sect. 72, 181–196. https://doi.org/10.1016/0168-9622(88)90066-8.
Ho, P., Shim, M.J., Howden, S.D., Shiller, A.M., 2019. Temporal and spatial distributions of nutrients and trace elements (Ba, Cs, Cr, Fe, Mn, Mo, U, V and Re) in Mississippi coastal waters: influence of hypoxia, submarine groundwater discharge, and episodic events. Cont. Shelf Res. 175, 53–69. https://doi.org/10.1016/j.csr.2019.01.013.
Hu, C., Muller-Karger, F.E., Swarzenski, P.W., 2006. Hurricanes, submarine groundwater discharge, and Florida's red tides. Geophys. Res. Lett. 33, L11601 https://doi.org/10.1029/2005GL025449.
Joung, D., Shiller, A.M., 2013. Trace element distributions in the water column near the Deepwater horizon well blowout. Environ. Sci. Technol. 47, 2161–2168. https://doi.org/10.1021/es303167p.
Joung, D., Shiller, A.M., 2014. Dissolved barium behavior in Louisiana Shelf waters affected by the Mississippi/Atchafalaya River mixing zone. Geochim. Cosmochim. Acta 141, 303–313. https://doi.org/10.1016/j.gca.2014.06.021.
Jouon, A., Douillet, P., Ouillon, S., Fraunié, P., 2006. Calculations of hydrodynamic time parameters in a semi-opened coastal zone using a 3D hydrodynamic model. Cont. Shelf Res. 26, 1395–1415. https://doi.org/10.1016/j.csr.2005.11.014 (Recent Developments in Physical Oceanographic Modelling: Part III).

Justić, D., Rabalais, N.N., Eugene Turner, R., Wiseman, W.J., 1993. Seasonal coupling between riverborne nutrients, net productivity and hypoxia. Mar. Pollut. Bull. 26, 184–189. https://doi.org/10.1016/0025-326X(93)90620-Y.

Justić, D., Rabalais, N.N., Turner, R.E., 2002. Modeling the impacts of decadal changes in riverine nutrient fluxes on coastal eutrophication near the Mississippi River Delta. Ecol. Model. 152, 33–46. https://doi.org/10.1016/S0304-3800(01)00472-0.

Kaul, L.W., Froelich, P.N., 1984. Modeling estuarine nutrient geochemistry in a simple system. Geochim. Cosmochim. Acta 48, 1417–1433. https://doi.org/10.1016/0016-7037(84)90399-5.

Kolker, A.S., Cable, J.E., Johannesson, K.H., Allison, M.A., Inniss, L.V., 2013. Pathways and processes associated with the transport of groundwater in deltaic systems. J. Hydrol. 498, 319–334. https://doi.org/10.1016/j.jhydrol.2013.06.014.

Kraemer, T.F., Reid, D.F., 1984. The occurrence and behavior of radium in saline formation water of the U.S. Gulf Coast region. Chem. Geol. 46, 153–174. https://doi.org/10.1016/0009-2541(84)90186-4.

Krest, J.M., Moore, W.S., Rama, 1999. 226Ra and 228Ra in the mixing zones of the Mississippi and Atchafalaya Rivers: indicators of groundwater input. Mar. Chem. 64, 129–152. https://doi.org/10.1016/S0304-4203(98)00070-X.

Kroeger, K.D., Swarzenski, P.W., Greenwood, Wm.J., Reich, C., 2007. Submarine groundwater discharge to Tampa Bay: nutrient fluxes and biogeochemistry of the coastal aquifer. Mar. Chem. 104, 85–97. https://doi.org/10.1016/j.marchem.2006.10.012 (Biogeochemical Cycles in Tampa Bay, Florida).

Lapointe, B.E., 1997. Nutrient thresholds for bottom-up control of macroalgal blooms on coral reefs in Jamaica and Southeast Florida. Limnol. Oceanogr. 42, 1119–1131. https://doi.org/10.4319/lo.1997.42.5_part_2.1119.

Liefer, J.D., MacIntyre, H.L., Su, N., Burnett, W.C., 2014. Seasonal alternation between groundwater discharge and benthic coupling as nutrient sources in a shallow coastal lagoon. Estuar. Coasts 37, 925–940. https://doi.org/10.1007/s12237-013-9739-4.

Macintyre, H.L., Stutes, A.L., Smith, W.L., Dorsey, C.P., Abraham, A., Dickey, R.W., 2011. Environmental correlates of community composition and toxicity during a bloom of Pseudo-nitzschia spp. in the northern Gulf of Mexico. J. Plankton Res. 33, 273–295. https://doi.org/10.1093/plankt/fbq146.

McCoy, C.A., Corbett, D.R., 2009. Review of submarine groundwater discharge (SGD) in coastal zones of the Southeast and Gulf Coast regions of the United States with management implications. J. Environ. Management 90, 644–651. https://doi.org/10.1016/j.jenvman.2008.03.002.

McCoy, C.A., Corbett, D.R., McKee, B.A., Top, Z., 2007. An evaluation of submarine groundwater discharge along the continental shelf of Louisiana using a multiple tracer approach. J. Geophys. Res. Oceans 112. https://doi.org/10.1029/2006JC003505.

McManus, J., Berelson, W.M., Klinkhammer, G.P., Johnson, K.S., Coale, K.H., Anderson, R.F., Kumar, N., Burdige, D.J., Hammond, D.E., Brumsack, H.J., McCorkle, D.C., Rushdi, A., 1998. Geochemistry of barium in marine sediments: implications for its use as a paleoproxy. Geochim. Cosmochim. Acta 62, 3453–3473. https://doi.org/10.1016/S0016-7037(98)00248-8.

Meinhold, A.F., Holtzman, S., DePhillips, M.P., 1996. Produced Water Discharges to the Gulf of Mexico: Background Information for Ecological Risk Assessments (No. BNL–63331). Brookhaven National Lab.

Montiel, D., Lamore, A., Stewart, J., Dimova, N., 2018. Is submarine groundwater discharge (SGD) important for the historical fish kills and harmful algal bloom events of Mobile Bay? Estuar. Coasts. https://doi.org/10.1007/s12237-018-0485-5.

Moore, W.S., 1976. Sampling radium-228 in the deep ocean. Deep-Sea Res. 23, 647–651.

Moore, W.S., 1984. Radium isotope measurements using germanium detectors. Nucl. Inst. Methods Phys. Res. A 223, 407–411. https://doi.org/10.1016/0167-5087(84)90683-5.

Moore, W.S., 2000. Determining coastal mixing rates using radium isotopes. Cont. Shelf. Res. 20, 1993–2007. https://doi.org/10.1016/S0278-4343(00)00054-6.

Moore, W.S., 2003. Sources and fluxes of submarine groundwater discharge delineated by radium isotopes. Biogeochemistry 66, 75–93. https://doi.org/10.1023/B:BIOG.0000006065.77764.a0.

Moore, W.S., 2008. Fifteen years experience in measuring ^{224}Ra and ^{223}Ra by delayed-coincidence counting. Mar. Chem. 109, 188–197. https://doi.org/10.1016/j.marchem.2007.06.015 (Measurement of Radium and Actinium Isotopes in the marine environment).

Moore, W.S., Arnold, R., 1996. Measurement of ^{223}Ra and ^{224}Ra in coastal waters using a delayed coincidence counter. J. Geophys. Res. Oceans 101, 1321–1329. https://doi.org/10.1029/95JC03139.

Moore, W.S., Krest, J., 2004. Distribution of ^{223}Ra and ^{224}Ra in the plumes of the Mississippi and Atchafalaya Rivers and the Gulf of Mexico. Mar. Chem. 86, 105–119. https://doi.org/10.1016/j.marchem.2003.10.001.

Moore, W.S., Reid, D.F., 1973. Extraction of radium from natural waters using manganese-impregnated acrylic fibers. J. Geophys. Res. 78, 8880–8886. https://doi.org/10.1029/JC078i036p08880.

Moore, W.S., Shaw, T.J., 2008. Fluxes and behavior of radium isotopes, barium, and uranium in seven southeastern US rivers and estuaries. Mar. Chem. 108, 236–254. https://doi.org/10.1016/j.marchem.2007.03.004.

Moore, W.S., Blanton, J.O., Joye, S.B., 2006. Estimates of flushing times, submarine groundwater discharge, and nutrient fluxes to Okatee Estuary, South Carolina. J. Geophys. Res. Oceans 111, C09006. https://doi.org/10.1029/2005JC003041.

Morey, S.L., Martin, P.J., O'Brien, J.J., Wallcraft, A.A., Zavala-Hidalgo, J., 2003. Export pathways for river discharged fresh water in the northern Gulf of Mexico. J. Geophys. Res. Oceans 108, 3303. https://doi.org/10.1029/2002JC001674.

Moshogianis, A., Lopez, J., Henkel, T., Boyd, E., Baker, A., Hillmann, E., 2013. Preliminary Results of Recently Observed Hypoxia Development in the Chandeleur Sound and Breton Sound of Southeastern Louisiana, East of the Mississippi River Delta (Technical Report). Lake Pontchartrain Basin Foundation.

Niemistö, J., Lund-Hansen, L.C., 2019. Instantaneous effects of sediment resuspension on inorganic and organic benthic nutrient fluxes at a shallow water coastal site in the Gulf of Finland, Baltic Sea. Estuar. Coasts 42, 2054–2071. https://doi.org/10.1007/s12237-019-00648-5.

Paerl, H.W., 1997. Coastal eutrophication and harmful algal blooms: importance of atmospheric deposition and groundwater as "new" nitrogen and other nutrient sources. Limnol. Oceanogr. 42, 1154–1165. https://doi.org/10.4319/lo.1997.42.5_part_2.1154.

Parra, S.M., Sanial, V., Boyette, A.D., Cambazoglu, M.K., Soto, I.M., Greer, A.T., Chiaverano, L.M., Hoover, A., Dinniman, M.S., 2020. Bonnet Carré Spillway freshwater transport and corresponding biochemical properties in the Mississippi Bight. Cont. Shelf Res. 199, 104114. https://doi.org/10.1016/j.csr.2020.104114.

Peterson, R.N., Moore, W.S., Chappel, S.L., Viso, R.F., Libes, S.M., Peterson, L.E., 2016. A new perspective on coastal hypoxia: the role of saline groundwater. Mar. Chem. 179, 1–11. https://doi.org/10.1016/j.marchem.2015.12.005.

Rabalais, N.N., Turner Jr., R.E., W.J.W, 2002. Gulf of Mexico Hypoxia, A.K.A. "The Dead Zone.". Annu. Rev. Ecol. Syst. 33, 235–263. https://doi.org/10.1146/annurev.ecolsys.33.010802.150513.

Rakocinski, C.F., Menke, D.P., 2016. Seasonal hypoxia regulates macrobenthic function and structure in the Mississippi Bight. Mar. Pollut. Bull. 105, 299–309. https://doi.org/10.1016/j.marpolbul.2016.02.006.

Rasheed, M., Wild, C., Franke, U., Huettel, M., 2004. Benthic photosynthesis and oxygen consumption in permeable carbonate sediments at Heron Island, Great Barrier Reef. Australia. Estuar. Coast. Shelf Sci. 59, 139–150. https://doi.org/10.1016/j.ecss.2003.08.013.

Reid, D.F., Moore, W.S., Sackett, W.M., 1979. Temporal variation of ^{228}Ra in the near-surface Gulf of Mexico. Earth Planet. Sci. Lett. 43, 227–236. https://doi.org/10.1016/0012-821X(79)90206-1.

Roberts, H.M., Shiller, A.M., 2015. Determination of dissolved methane in natural waters using headspace analysis with cavity ring-down spectroscopy. Anal. Chim. Acta 856, 68–73. https://doi.org/10.1016/j.aca.2014.10.058.

Rodellas, V., Garcia-Orellana, J., Masqué, P., Feldman, M., Weinstein, Y., 2015a. Submarine groundwater discharge as a major source of nutrients to the Mediterranean Sea. Proc. Natl. Acad. Sci. 112, 3926–3930. https://doi.org/10.1073/pnas.1419049112.

Rodellas, V., Garcia-Orellana, J., Masqué, P., Font-Muñoz, J.S., 2015b. The influence of sediment sources on radium-derived estimates of Submarine Groundwater Discharge. Mar. Chem. 171, 107–117. https://doi.org/10.1016/j.marchem.2015.02.010.

Rodellas, V., Garcia-Orellana, J., Trezzi, G., Masqué, P., Stieglitz, T.C., Bokuniewicz, H., Cochran, J.K., Berdalet, E., 2017. Using the radium quartet to quantify submarine groundwater discharge and porewater exchange. Geochim. Cosmochim. Acta 196, 58–73. https://doi.org/10.1016/j.gca.2016.09.016.

Sanial, V., Shiller, A., Joung, D.J., Ho, P., 2019. Extent of Mississippi River water in the Mississippi Bight and Louisiana Shelf based on water isotopes. Estuar. Coast. Shelf Sci. https://doi.org/10.1016/j.ecss.2019.04.030.

Santos, I.R., Eyre, B.D., Huettel, M., 2012. The driving forces of porewater and groundwater flow in permeable coastal sediments: a review. Estuar. Coast. Shelf Sci. 98, 1–15. https://doi.org/10.1016/j.ecss.2011.10.024.

Selman, M., Greenhalgh, S., Diaz, R., Sugg, Z., 2008. Eutrophication and Hypoxia in Coastal Areas, Policy Note, Water Quality: Eutrophication and Hypoxia, 1st ed. World Resource Institute, Washington, D. C.

Shaw, T.J., Moore, W.S., Kloepfer, J., Sochaski, M.A., 1998. The flux of barium to the coastal waters of the southeastern USA: the importance of submarine groundwater discharge. Geochim. Cosmochim. Acta 62, 3047–3054. https://doi.org/10.1016/S0016-7037(98)00218-X.

Shiller, A.M., 1996. The effect of recycling traps and upwelling on estuarine chemical flux estimates. Geochim. Cosmochim. Acta 60, 3177–3185. https://doi.org/10.1016/0016-7037(96)00159-7.

Shiller, A.M., 1997. Dissolved trace elements in the Mississippi River: seasonal, interannual, and decadal variability. Geochim. Cosmochim. Acta 61, 4321–4330. https://doi.org/10.1016/S0016-7037(97)00245-7.

Shiller, A.M., 2003. Syringe filtration methods for examining dissolved and colloidal trace element distributions in remote field locations. Environ. Sci. Technol. 37, 3953–3957. https://doi.org/10.1021/es0341182.

Shiller, A.M., Box, H., Gilbert, M., Joung, D.J., Sanial, V., 2019. Chemical data for rivers influencing the Mississippi Bight from 2015-10-01 to 2016-06-08. In: Distributed by: Gulf of Mexico Research Initiative Information and Data Cooperative (GRIIDC). Harte Research Institute, Texas A&M University, Corpus Christi. https://doi.org/10.7266/n7-sps7-rq23.

Shim, M.-J., Swarzenski, P.W., Shiller, A.M., 2012. Dissolved and colloidal trace elements in the Mississippi River delta outflow after Hurricanes Katrina and Rita. Cont. Shelf Res. 42, 1–9. https://doi.org/10.1016/j.csr.2012.03.007.

Slomp, C.P., Van Cappellen, P., 2004. Nutrient inputs to the coastal ocean through submarine groundwater discharge: controls and potential impact. J. Hydrol. 295, 64–86. https://doi.org/10.1016/j.jhydrol.2004.02.018.

Smoak, J.M., DeMaster, D.J., Kuehl, S.A., Pope, R.H., McKee, B.A., 1996. The behavior of particle-reactive tracers in a high turbidity environment: ^{234}Th and ^{210}Pb on the Amazon continental shelf. Geochim. Cosmochim. Acta 60, 2123–2137. https://doi.org/10.1016/0016-7037(96)00092-0.

Solórzano, L., Sharp, J.H., 1980. Determination of total dissolved nitrogen in natural waters1. Limnol. Oceanogr. 25, 751–754. https://doi.org/10.4319/lo.1980.25.4.0751.

Spalt, N., Murgulet, D., Hu, X., 2018. Relating estuarine geology to groundwater discharge at an oyster reef in Copano Bay, TX. J. Hydrol. 564, 785–801. https://doi.org/10.1016/j.jhydrol.2018.07.048.

Sun, Y., Torgersen, T., 1998. The effects of water content and Mn-fiber surface conditions on ^{224}Ra measurement by 220Rn emanation. Mar. Chem. 62, 299–306. https://doi.org/10.1016/S0304-4203(98)00019-X.

Taylor, P., 1995. Interactions of Silica with Iron Oxides: Effects on Oxide Transformations and Sorption Properties (No. AECL–11257). Atomic Energy of Canada Ltd.

Vaquer-Sunyer, R., Duarte, C.M., 2008. Thresholds of hypoxia for marine biodiversity. Proc. Natl. Acad. Sci. 105, 15452–15457. https://doi.org/10.1073/pnas.0803833105.

Veil, J.A., Kimmell, T.A., Rechner, A.C., 2005. Characteristics of Produced Water Discharged to the Gulf of Mexico hypoxiczone. (No. ANL/EAD/05-3). Argonne National Lab. (ANL), Argonne, IL (United States). https://doi.org/10.2172/861623.

Walker, N.D., Wiseman, W.J., Rouse, L.J., Babin, A., 2005. Effects of river discharge, wind stress, and slope eddies on circulation and the satellite-observed structure of the Mississippi River Plume. J. Coast. Res. 216, 1228–1244. https://doi.org/10.2112/04-0347.1.

Warner, J.C., Armstrong, B., He, R., Zambon, J.B., 2010. Development of a coupled ocean–atmosphere–wave–sediment transport (COAWST) modeling system. Ocean Model 35, 230–244. https://doi.org/10.1016/j.ocemod.2010.07.010.

Zhang, Z., Falter, J., Lowe, R., Ivey, G., 2012. The combined influence of hydrodynamic forcing and calcification on the spatial distribution of alkalinity in a coral reef system. J. Geophys. Res. Oceans 117. https://doi.org/10.1029/2011JC007603.

Zimmerman, M.J., Massey, A.J., Campo, K.W., 2005. Pushpoint sampling for defining spatial and temporal variations in contaminant concentrations in sediment pore water near the ground-water/surface-water interface, Scientific Investigations Report 2005-5036. US Geological Survey 70. https://pubs.usgs.gov/sir/2005/5036/.